Developmental Biology 340 (2010) 490–503

Contents lists available at ScienceDirect

Developmental Biology

journal homepage: www.elsevier.com/developmentalbiology

Neurog2 controls the leading edge of neurogenesis in the mammalian retina

Robert B. Hufnagel, Tien T. Le, Ashley L. Riesenberg, Nadean L. Brown *

Division of Developmental Biology, Cincinnati Children's Research Foundation, Departments of Pediatrics and Ophthalmology, University of Cincinnati College of Medicine, Cincinnati, OH 45229, USA

ARTICLE INFO

Article history:
Received for publication 17 September 2009
Revised 20 January 2010
Accepted 1 February 2010
Available online 6 February 2010

Keywords:
Neurog2
Atoh7
Ascl1
Retinal ganglion cell
Retina
Neurogenesis

ABSTRACT

In the mammalian retina, neuronal differentiation begins in the dorso-central optic cup and sweeps peripherally and ventrally. While certain extrinsic factors have been implicated, little is known about the intrinsic factors that direct this process. In this study, we evaluate the expression and function of proneural bHLH transcription factors during the onset of mouse retinal neurogenesis. Dorso-central retinal progenitor cells that give rise to the first postmitotic neurons express *Neurog2*/*Ngn2* and *Atoh7*/*Math5*. In the absence of *Neurog2*, the spread of neurogenesis stalls, along with *Atoh7* expression and RGC differentiation. However, neurogenesis is eventually restored, and at birth *Neurog2* mutant retinas are reduced in size, with only a slight increase in the retinal ganglion cell population. We find that the re-establishment of neurogenesis coincides with the onset of *Ascl1* expression, and that *Ascl1* can rescue the early arrest of neural development in the absence of *Neurog2*. Together, this study supports the hypothesis that the intrinsic factors *Neurog2* and *Ascl1* regulate the temporal progression of retinal neurogenesis by directing overlapping waves of neuron formation.

Introduction

Visual processing in the retina depends on proper functioning of multiple neural classes. Thus, determining how this neuronal diversity arises is critical for understanding retinal function. Seven major retinal cell classes are generated between embryonic day (E) 11 and postnatal day (P) 10 in the mouse, in a conserved temporal order (Sidman, 1961; Young, 1985). In vertebrates, retinal ganglion cells (RGCs) differentiate first, as a wave front across the neuroepithelium of the optic cup (Easter, 2000; Holt et al., 1988; Masai et al., 2000; McCabe et al., 1999). In zebrafish, this wave begins near the optic stalk and radiates outward (Hu and Easter, 1999). In avians, the first RGCs appear in the dorsal–central retina, and neurogenesis simultaneously spreads peripherally and ventrally (Prada et al., 1991). Multiple extrinsic signals, including FGFs and sonic hedgehog, are required for the spatiotemporal progression of retinal neurogenesis (Jensen and Wallace, 1997; Macdonald et al., 1995; Martinez-Morales et al., 2005; McCabe et al., 1999; Neumann and Nuesslein-Volhard, 2000; Perron et al., 2003; Picker and Brand, 2005). However, little is known about the intrinsic factors that regulate this process.

The basic-helix–loop–helix (bHLH) transcription factors, including *Atoh7*/*Ath5*, *Ascl1*/*Ash1*, *Neurog2*/*Ngn2*, and *Neurod1*, regulate multiple facets of neurogenesis, including cell cycle exit, neural versus glial determination, subtype specification, and survival (Ohsawa and Kageyama, 2008). Among the first proneural bHLHs expressed in the vertebrate retina, *Atoh7* (*atonal* homologue 7) appears at the onset of retinal neurogenesis in the dorso-central mouse retina, and loss-of-function mutations result in the reduced differentiation of early progenitor cells and nearly complete loss of RGCs (Brown et al., 1998, 2001; Kanekar et al., 1997; Kay et al., 2001; Matter-Sadzinski et al., 2001; Wang et al., 2001). The vertebrate bHLH factor, *Neurog2* (also an *atonal* homologue) is expressed during early retinogenesis (Brown et al., 1998; Ma and Wang, 2006). In the chick eye, *Neurog2* can genetically activate *Atoh7* and transdifferentiate cultured RPE cells into immature RGCs and photoreceptors (Matter-Sadzinski et al., 2005; Yan et al., 2001). By contrast, *X-ngnr-1*, a *Xenopus Neurog2* homologue, promotes photoreceptor but not RGC formation (Perron et al., 1999). Recently, Neurog2/Ngn2 was demonstrated to bind to 5′ regulatory DNA and activate *Atoh7*/*Ath5* transcription using distinct species-specific mechanisms in the mouse versus chick retina (Skowronska-Krawczyk et al., 2009). However, no individual role for *Neurog2* has been uncovered, particularly in the mammalian retina (Akagi et al., 2004; Skowronska-Krawczyk et al., 2009).

In this report, we investigate intrinsic elements controlling the spatial and temporal onset of retinal neurogenesis, and define a novel role for *Neurog2* during the outward expansion of retinal neurogenesis. *Neurog2* and *Atoh7* are simultaneously activated in cells that give rise to the first RGCs. *Neurog2* is required for the spatial and temporal progression of both the expanding wave front and *Atoh7* expression, but the resulting delay of neurogenesis is transient. The onset of *Ascl1*, a later-expressed bHLH factor, coincides with the restoration of retinal neurogenesis, and rescues neural differentiation in the absence of

* Corresponding author. Division of Developmental Biology, Cincinnati Children's Research Foundation, USA. Fax: +1 513 636 4317.
E-mail address: Nadean.Brown@cchmc.org (N.L. Brown).

0012-1606/$ – see front matter © 2010 Elsevier Inc. All rights reserved.
doi:10.1016/j.ydbio.2010.02.002

Neurog2. Together, these data demonstrate a critical role for bHLH factors in both propagating and maintaining the spatial and temporal progression of mammalian retinogenesis.

Materials and methods

Animals

Neurog2^{GFP} mice (Seibt et al., 2003) were maintained on an ICR background, and *Atoh7*^{LacZ} (Brown et al., 2001), Ascl1$^{KO/+}$ (Tomita et al., 1996) and *Neurog2*^{Ascl1KI} mice (Fode et al., 2000) on a CD-1 background. For double-mutant studies, mice were bred together for a minimum of two generations. PCR genotyping was performed as described (Brown et al., 2001; Fode et al., 2000; Seibt et al., 2003; Tomita et al., 1996).

For embryonic studies, gestational age was determined by timed matings, with the date of the vaginal plug as E0.5. For somite-counted embryos, 4–6 h timed matings were carried out to precisely correlate somite number with gestational age. BrdU pulse-labeling was performed by injecting pregnant dams with BrdU (0.1 mg/g body weight of 10 mg/mL BrdU in 0.9 M NaCl) and harvesting embryos after 1.5 h. P0.5 pups were collected on the morning after birth.

Immunohistochemistry and in situ hybridization

Immunohistochemistry was performed as described (Hufnagel et al., 2007). Antibodies used were rabbit anti-βIII-tubulin (Tubb3) (1:1000, Covance), rabbit anti-βgal (1:10,000, Cappel), rat anti-βgal (1:1000, gift from Tom Glaser), rat anti-BrdU (1:100, AbD Serotec), goat anti-Pou4f2/Brn3b (1:50, Santa Cruz), rabbit anti-activated Caspase 3 (1:100, Cell Signaling), sheep anti-Chx10 (1:1000, Exalpha Biologicals), rabbit anti-GFP (1:1000, Molecular Probes), rabbit anti-Ascl1 (1:1000; Horton et al., 1999), rabbit anti-Neurog1 (1:1000, Gowan et al., 2001), rabbit anti-Neurog2 (1:1000), mouse anti-Neurog2 (1:10, Lo et al., 2002), mouse anti-Neurog3 (1:100, DSHB), mouse anti-p27 (1:200, Thermo scientific), rabbit anti-Pax6 (1:1000, Covance), rabbit anti-Pax2 (1:1000, Covance), mouse anti-AP2α (1:500, DSHB), rabbit anti-Prox1 (1:1000, Covance), rabbit anti-RXRγ (1:200, Santa Cruz), and rabbit anti-Sox2 (1:1000, Chemicon). Direct-conjugate secondary antibodies (Molecular Probes) or sequential biotinylated secondary (Jackson Immunoresearch) and streptavidin-conjugated Alexafluor tertiary antibodies (Molecular Probes) were used to visualize primary antibody labeling.

In situ hybridization was performed as described (Wallace and Raff, 1999). Briefly, embryos were collected and fixed in 4% PFA/PBS overnight, then cryoprotected in 30% sucrose overnight, embedded in 50:50 OCT:30% sucrose, and sectioned at a thickness of 10 μm. DIG-labeled antisense *Atoh7*, *Ascl1*, and *Neurod1* probes were hybridized to retinal sections overnight, detected with sheep anti-DIG antibody (1:2000; Roche), and developed with NBT and BCIP.

Measurements and cell counting

Microscopy was performed with a Zeiss fluorescent microscope, Zeiss camera and Apotome deconvolution device. For all retinal measurements or cell counts, a minimum of 3 embryos or postnatal pups per genotype from ≥2 independent litters were analyzed, matched for somite number across genotypes. Cell counts and measurements were performed using the Zeiss Axiovision software (v5.0), using the interactive events and curve spline tools. The circumference of the Tubb3 expression was compared to the circumference of the Neurog2-GFP domain and the total outer circumference from 4 images per animal, representing both eyes, containing the optic nerve or within 50 μm dorsal to the optic nerve. The percentages of BrdU+/DAPI, act Caspase+/DAPI, RXRγ+/DAPI, Pou4f2+/DAPI, AP2α+/DAPI, Prox1+/DAPI nuclei were determined in 200× fields within in the central retina. Either a paired Student's *T* test with Welch posthoc test or ANOVA with Tukey–Kramer posthoc test was used to determine *n* values (Instat Software, v3.0). Photoshop (v7.0) was used to adjust equally the brightness and contrast of images among different genotypes.

Results

Comparison of Ngn2 and Atoh7 expression during early retinogenesis

During the initiation of retinal neurogenesis, progenitor cells exit the cell cycle, express general neuronal markers, and commit to a single cell fate. Among vertebrates, RGCs appear first (Altshuler et al., 1991), initially in the dorso-central retina of avians and mammals. In the chick retina, neurogenesis spreads in simultaneous central–peripheral and dorsal–ventral gradients, and is regulated partly by FGF signaling (McCabe et al., 1999; Prada et al., 1991). An analogous wave front in the mammalian retina has not been described, so we sought to understand the spatiotemporal kinetics of this process in the mouse eye, and test the hypothesis that bHLH factors *Neurog2*/*Ngn2* and/or *Atoh7*/*Math5* regulate the initial neurogenic wave.

The first *Atoh7*-expressing cells are found in the dorso-central retina at E11.0, preceding the appearance of RGCs that critically require this factor (Brown et al., 1998; Brown et al., 2001; Wang et al., 2001). *Neurog2* expression has also been reported to appear around the time of neurogenesis initiation in the early chick and mouse retina (Ma and Wang, 2006; Matter-Sadzinski et al., 2005). First, we compared the expression pattern of *Neurog2*/*Ngn2* to *Atoh7*/*Math5* and the initial spread of retinal neuron differentiation. To correlate *Neurog2* and *Atoh7* expression directly, we assessed the onset of *Atoh7*^{LacZ} with that of *Neurog2*^{GFP} and Neurog2 protein expression (Brown et al., 2001; Seibt et al., 2003), by antibody double labeling of retina sections from double-heterozygous animals (*Neurog2*$^{GFP/+}$; *Atoh7*$^{LacZ/+}$ mice; Figs. 1A,B), which are identical to wild types (not shown). Brief timed matings (4–6 h) were used to precisely correlate gestational ages of somite-counted E10.75–E12.0 embryonic litters. Prior to E11.0, Neurog2 protein and *Neurog2*^{GFP} expression were localized to the ventral thalamus and presumptive optic stalk, but excluded from the retina (Fig. 1C and data not shown). The earliest retinal Neurog2+ and GFP+ cells were found at E11.0 in the dorso-central retina (43 somites, Figs. 1E,E'). From E11.0–E11.5 (43–50 somites), 6 of 11 embryos contained both Neurog2+ and *Neurog2*^{GFP}+ cells, indicating that retinal onset of *Neurog2* does not precisely correlate with somite number. All embryonic retinas at E11.75 (51–60 somites) contained Neurog2+/GFP+ cells.

Next, we asked if the onset of *Neurog2* or *Atoh7* expression precedes the other. We performed antibody labeling in double-heterozygous mice (*Neurog2*$^{GFP/+}$;*Atoh7*$^{LacZ/+}$) and *Atoh7* mutants (*Neurog2*$^{GFP/+}$;*Atoh7*$^{LacZ/LacZ}$), since bi-allelic expression of *Atoh7*^{LacZ} enhanced the detection of βgal+ cells. We do not observe either *Neurog2*^{GFP}+ or βgal+ retinal cells prior to 43 somites (Fig. 1D), although co-labeled GFP+ and βgal+ cells were noted in the diencephalon (arrow, Fig. 1D). *Neurog2*^{GFP} and *Atoh7*^{LacZ} were extensively co-expressed in the mouse dorso-central retina at E11.0 (arrows, Figs. 1F,G). At E11.75 and E12.5, both *Neurog2* and *Atoh7* expression had expanded peripherally, with a bias towards the temporal/caudal retina (Figs. 1H,I). The *Neurog2*^{GFP} domain always extended more peripherally and encompassed more cells than the *Atoh7*^{LacZ} domain (GFP+/βgal− region in brackets, Fig. 1I). At all ages examined, virtually all βgal+ cells were also GFP+ (arrows, Figs. 1F–I), indicating *Atoh7*^{LacZ} was expressed in a subset of *Neurog2*^{GFP}+ cells.

To further examine the coincidence between *Neurog2* and *Atoh7*, we compared the pattern of Neurog2 protein with *Atoh7*^{LacZ} and *Neurog2*^{GFP}. Neurog2 is largely present in S-phase progenitor cells (Fig. 1K; Ma and Wang, 2006; Yan et al., 2001). *Atoh7*/*Ath5* is not expressed during S-phase (Fig. 1J) (Le et al., 2006; Poggi et al., 2005),

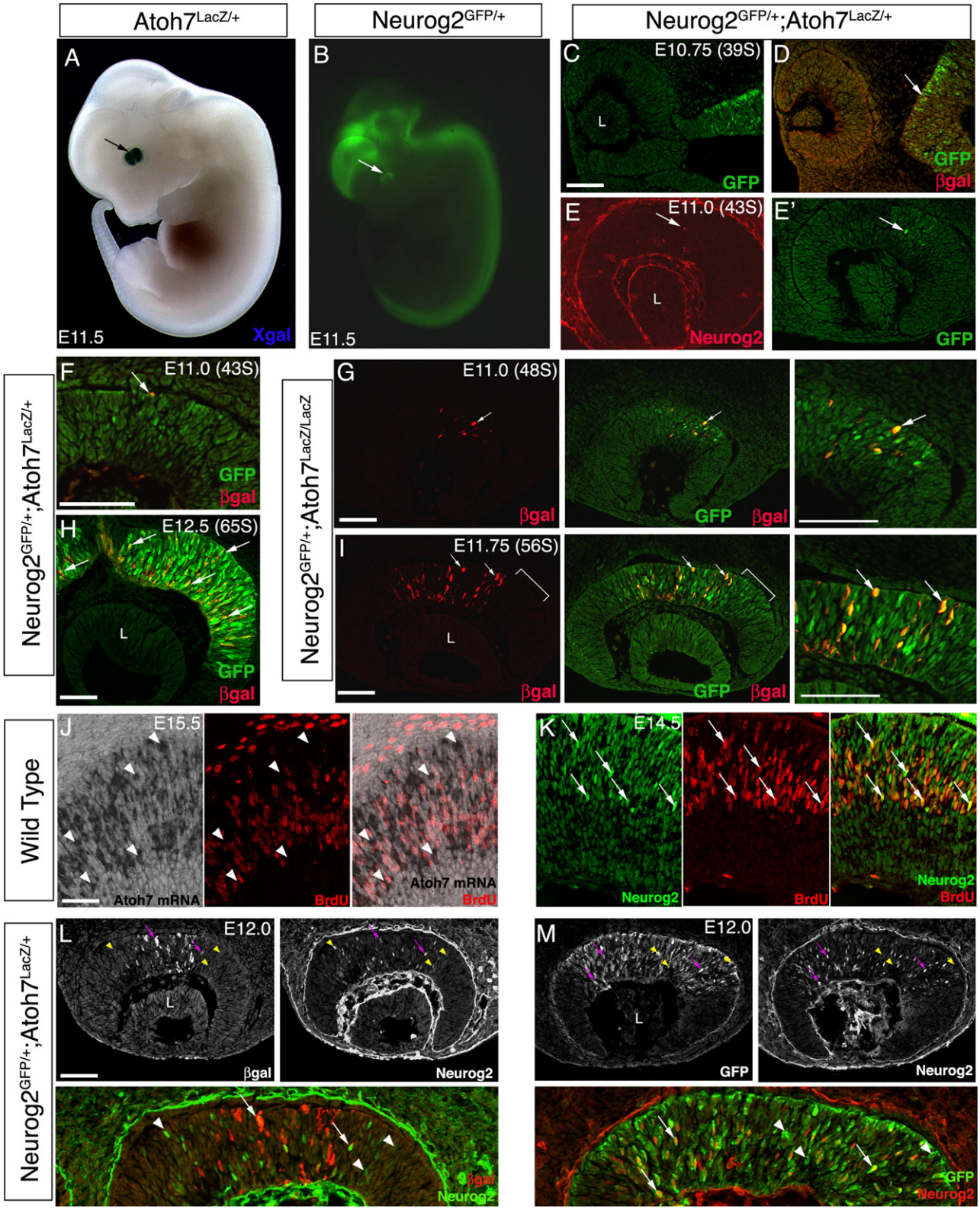

Fig. 1. Onset of Neurog2 protein, *Neurog2*^{GFP} and *Atoh7*^{LacZ} expression in the mouse retina. A–B) Whole mount micrographs of *Atoh7*$^{LacZ/+}$ and *Neurog2*$^{GFP/+}$ embryos at E11.5, demonstrated retinal expression for each reporter (arrows). C–D) Immunolabeling for GFP and βgal showed no detectable optic cup expression at E10.75, although coexpressing cells were present in the diencephalon (arrow in D). E–H) Labeling of Neurog2 protein and GFP at onset of neurogenesis. GFP versus βgal at E11.0 (F) and E12.5 (H) in *Neurog2*$^{GFP/+}$; *Atoh7*$^{LacZ/+}$ mice showed consistent overlap of reporters at these ages. G,I) *Neurog2*$^{GFP/+}$;*Atoh7*$^{LacZ/LacZ}$ embryos double-labeled for GFP and βgal at E11.0 and E11.75, respectively, demonstrated the temporal progression of each expression domain. Arrows point to double-labeled cells, and brackets show *Neurog2*^{GFP} expression peripheral to the *Atoh7*^{LacZ} domain. J) There was no expression of *Atoh7* mRNA (arrowheads point to cells with purple in situ reaction product) observed in BrdU pulse-labeled retinal (red) cells. K) However, Neurog2 protein was clearly detected in many BrdU+S-phase cells at E11.75 and E14.5 (arrows). L) Most βgal+ cells were Neurog2+/βgal+ (fuchsia arrows). Yellow arrowheads mark Neurog2+/βgal− cells peripheral to the *Atoh7*^{LacZ} domain. M) The overlap of Neurog2 and GFP (fuchsia arrows) versus GFP+/Neurog2− cells (yellow arrowheads). Scale bars: 50 μm in C,G,H,L,J; 25 μm in F. L = lens.

and has been extensively reported to be expressed by late G2/M phase and postmitotic retinal cells (Brown et al., 1998; Le et al., 2006, Brzezinski, 2005; Yang et al, 2003). This implies that, in mitotically active retinal progenitor cells, *Neurog2* expression in S-phase precedes that of *Atoh7*. Consistent with this difference, very few cells co-labeled with Neurog2 and βgal proteins (fuchsia and white arrows, Fig. 1L). The extensive overlap of *Neurog2*^{GFP} and *Atoh7*^{LacZ} likely occurs because *Neurog2*^{GFP} persists longer than Neurog2 protein, thereby acting as a short-term lineage tracer (Britz et al., 2006). Indeed, while all Neurog2+ cells co-express *Neurog2*^{GFP} (fuchsia and white arrows, Fig. 1M), many GFP+/Neurog2− cells are present (yellow and white arrowheads, Fig. 1M). We conclude that *Neurog2* and *Atoh7* simultaneously initiate expression in dorsal–central retinal progenitor cells at E11.0, but at distinct phases of the mitotic cell cycle.

Neurog2^{GFP} *precedes the expansion of neurogenesis and RGC specification*

Prior to retinogenesis, the optic vesicle becomes compartmentalized into the neural retina, RPE, and optic stalk. Optic vesicle cells initially co-express the paired-homeobox transcription factors *Pax6* and *Pax2* (Baumer et al., 2003; Schwarz et al., 2000). *Pax2* is subsequently downregulated in the neural retina, but not *Pax6* (Baumer et al., 2003). Importantly, *Pax6* directly activates *Atoh7* and *Neurog2* (Marquardt et al., 2001; Riesenberg et al., 2009; Willardsen et al., 2009). Before the onset of *Neurog2*^{GFP} expression from E11.0–11.5, Pax2+ cells were detected throughout the optic cup and stalk (Fig. 2A). By E11.75, after *Neurog2*^{GFP} onset in the retina, Pax2 protein was restricted to the optic stalk and central–nasal optic cup, in GFP-negative cells (Figs. 2B,C). The *Neurog2*^{GFP} domain bordered that of *Pax2*, and very few GFP+/Pax2+ cells were noted (arrow, Fig. 2C). Therefore, *Pax2* downregulation precedes the initiation of *Neurog2* expression in the presumptive neural retina. This pattern of *Pax2* expression was unchanged in *Neurog2* mutants (not shown), indicating that *Neurog2* does not suppress *Pax2* retinal expression. Pax6 protein was co-expressed with all GFP+ cells at this age (Fig. 2D). *Neurog2*^{GFP} also co-localized with Sox2 and Chx10/Vsx2 proteins (not shown), two other transcription factors required for normal retinal progenitor differentiation (Burmeister et al., 1996; Taranova et al., 2006).

Next, we directly compared *Neurog2*^{GFP} expression with the onset and expansion of retinal neuron differentiation. Co-labeling for GFP and Tubb3 (βIII-Tubulin), a neural-specific marker (Brittis et al., 1995; Lee et al., 1990), revealed no differentiating retinal neurons prior to *Neurog2*^{GFP} onset (Fig. 2E). Pou4f2/Brn3b, a marker of specified RGCs (Xiang et al., 1993), and p27/Kip1, a cyclin-dependent kinase inhibitor that promotes cell cycle exit of retinal progenitor cells (Dyer and Cepko, 2001; Levine et al., 2000), were also absent prior to

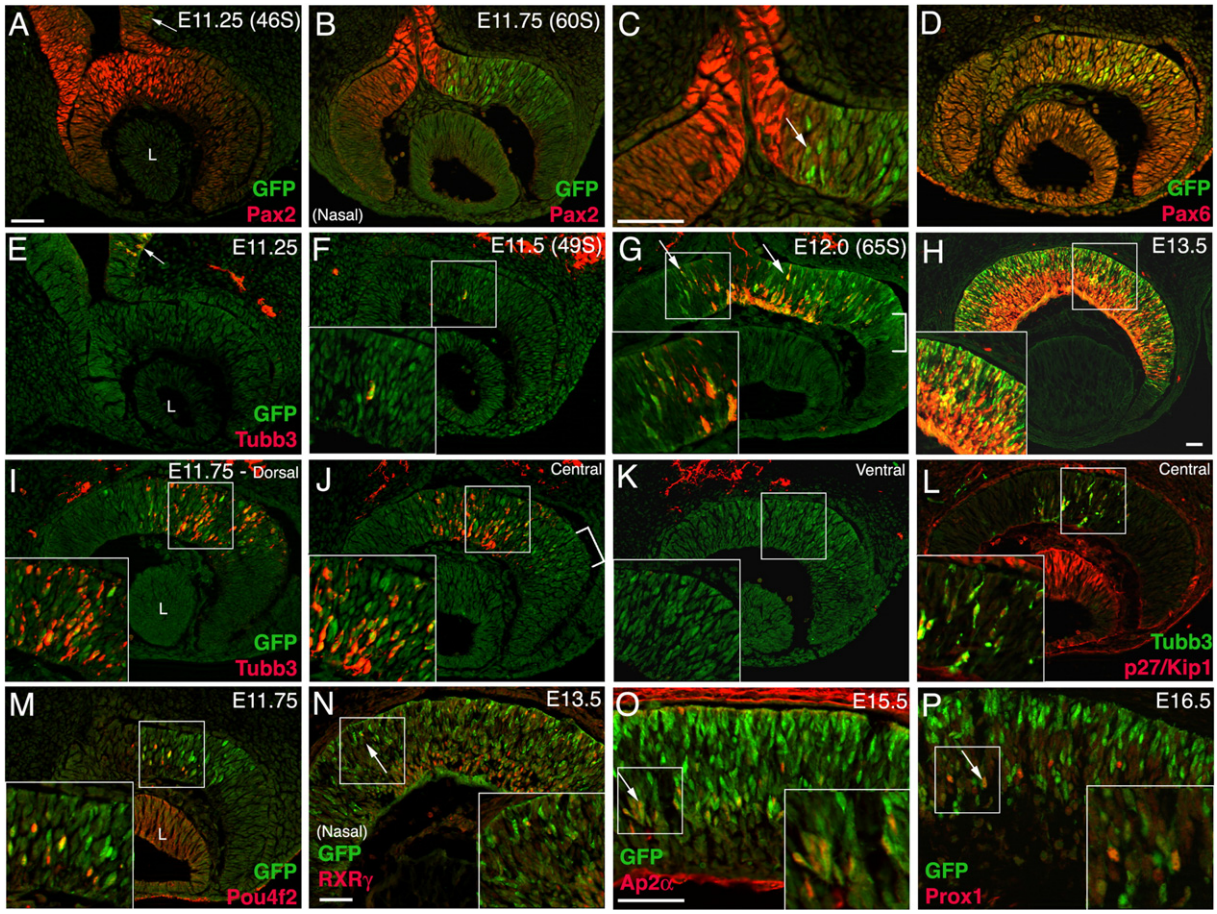

Fig. 2. Initiation of both retinal neurogenesis and *Neurog2*^{GFP} expression are coincident in the mouse eye. (A–C) Pax2 and *Neurog2*^{GFP} co-labeling. At E11.0–E11.5, Pax2+ cells are evident in the optic cup (A). When *Neurog2*^{GFP}+ cells first appeared in the central retina, the *Pax2* domain was restricted to the optic stalk and nasal retina (B,C). Arrow in C marks a very rare co-labeled *Neurog2*^{GFP}+/Pax2+ cell. (D) Extensive *Neurog2*^{GFP} coexpression with Pax6 protein. (E–H) Time course of the onset and expansion of neurogenesis and *Neurog2*^{GFP} expression. (E) In an E11.25 retina, *Neurog2*^{GFP}+/Tubb3+ cells were detected in the diencephalon, but not in the optic cup. (F) The first neurons appear from E11.0–E11.5 in *Neurog2*^{GFP}+ cells. (G) *Neurog2*^{GFP}+/Tubb3+ cells are present in the nasal and temporal retina at E12.0. Brackets indicate GFP+/Tubb3− domain. (H) By E13.5, the GFP and Tubb3 expression domains had reached the peripheral retina. (I–K) Dorsal, central, and ventral sections from the same eye at E11.75, demonstrating *Neurog2*^{GFP}+/Tubb3+ cells in the dorsal and central (I,J), but not ventral retina (K). (L) Tubb3 and p27/Kip1 were extensively co-expressed in cells exiting the cell cycle. (M) Pou4f2/Brn3b expression onsets at E11.75 in *Neurog2*^{GFP}+ cells. (N–P) GFP+ cells co-express markers of other embryonic fates: RXRγ+ cones (N), AP2α+ amacrines (O), and Prox1+ horizontal and amacrine interneurons (P). Scale bars: 50 μm in A,C,H,N,O. Insets in F–P are 8× magnifications of boxed area in each panel. L = lens.

Neurog2 onset (not shown). From E11.0–11.5, the first Tubb3+ and p27+ cells were detected in *Neurog2*^{GFP}+ retinal cells (Fig. 2F and not shown). By E11.75, the Tubb3 domain extended from the dorsal to central retina (Figs. 2I,J) but was not present ventral to the forming optic nerve (Fig. 2K). From E12.0–E13.5, the Tubb3+ region expanded peripherally and ventrally, with bias towards the temporal retina (Figs. 2G,H). The spread of the *Neurog2* domain preceded that of neural differentiation, indicated by the peripheral subdomain of GFP+/Tubb3− cells (brackets, Figs. 2G,J), which likely represents proliferating cells that subsequently differentiate into retinal neurons. Differentiating neurons highly co-expressed Tubb3 and p27 (Fig. 2L), verifying the concurrence of cell cycle exit and neural differentiation in the earliest retinal neurons. Essentially all Tubb3+ and p27+ cells co-labeled with *Neurog2*^{GFP} (Figs. 2F–J and not shown). At E11.75, the first GFP+/Pou4f2+ RGCs were detected in the dorso-central retina, proximal to the leading edges of the *Neurog2*^{GFP} and Tubb3 domains (Fig. 2M and not shown). No Pou4f2+ cells were detected prior to E11.75 (not shown). We conclude that the onset and peripheral expansion of *Neurog2* expression precedes the initiation of neurogenesis and subsequent differentiation of the first RGCs.

From E11.0–E13.5, neurogenesis spreads outward across the neural retina, excluding the optic nerve head and peripheral retina that give rise to the ciliary body and iris (Rodieck, 1998). Since *Neurog2* expression correlates with the onset of neural differentiation, we predicted that *Neurog2* expression would only be present in cells undergoing retinal neurogenesis. From E13.5 to birth, *Neurog2*^{GFP} co-localizes with Tubb3+ cells in the neuroblastic layer (NBL) and the inner forming ganglion cell layer (GCL), excluding the optic nerve head and presumptive ciliary body (Figs. 2H, 4B–C and not shown). Previous analysis of the *Neurog2*-lineage revealed that *Neurog2*-expressing cells are capable of adopting all the retinal fates (Ma and Wang, 2006). While that study found RGCs arise from the *Neurog2*-lineage starting at E14, here we found GFP+/Pou4f2+ RGCs much earlier, at E11.75 (Fig. 2M), suggesting that *Neurog2*^{GFP} acts as a short-term lineage tracer without the delay of Cre-mediated reporter activation by *Neurog2*^{CreER} (Ma and Wang, 2006). We then compared GFP expression with markers of other embryonic retinal cell types: cones (RXRγ), horizontals (Prox1), and amacrines (AP2α) (Dyer et al., 2003; Mori et al., 2001; Yan and Wang, 2004). RXRγ+/GFP+ cone photoreceptors were detected in the outer retina at E13.5 (arrows, Fig. 2N), also with a bias for the temporal retina. GFP+ amacrine (Ap2α+) and horizontal (Prox1+) interneurons were also noted in the prenatal retina (Figs. 2O,P and data not shown).

Neurog2 is required for the peripheral expansion of retinal neurogenesis

Neurog2 expression at the leading edge of retinal neurogenesis precedes the expansion of *Atoh7*, neural commitment, and RGC differentiation. Therefore, we asked if *Neurog2* is required for the peripheral propagation of neural development. GFP is still expressed in the absence of *Neurog2* (*Neurog2*$^{GFP/GFP}$, Fig. 3B), and marks the lineage of *Neurog2*-mutant cells. Thus, *Neurog2*^{GFP} allows for comparison of the peripheral extent of reporter-expressing cells (GFP+ domain) and nascent neurons (Tubb3+ domain) in heterozygous (*Neurog2*$^{GFP/+}$) and mutant (*Neurog2*$^{GFP/GFP}$) retinas. To confirm that the size of the GFP domain is not different for single or bi-allelic GFP expression, we compared the GFP domain relative to the total retinal circumference in *Neurog2*$^{GFP/+}$ and *Neurog2*$^{GFP/GFP}$ and found no difference between genotypes (Fig. 3H; see Materials and methods for description of domain measurements).

To determine whether the loss of *Neurog2* and/or *Atoh7* affects the ventral–peripheral expansion of retinal neurogenesis, we examined double-heterozygote controls (*Neurog2*$^{GFP/+}$;*Aoth7*$^{LacZ/+}$), *Neurog2* single-mutant (*Neurog2*$^{GFP/GFP}$;*Atoh7*$^{LacZ/+}$), *Atoh7* single-mutant (*Neurog2*$^{GFP/+}$;*Atoh7*$^{LacZ/LacZ}$), and double-mutant (*Neurog2*$^{GFP/GFP}$;*Atoh7*$^{LacZ/LacZ}$) retinas. The double-heterozygotes are appropriate controls since *Atoh7* heterozygotes have no phenotypes compared to wild types (Brown et al., 2001; Le et al., 2006; Wang et al., 2001), and both *Neurog2*$^{GFP/+}$ and *Neurog2*$^{GFP/+}$;*Atoh7*$^{LacZ/+}$ retinas exhibited no significant differences from wild type eyes (not shown).

First, we evaluated the expansion of Tubb3+ cells in relation to the *Neurog2*^{GFP} domain in somite-matched embryos at E11.75 (54–60 somites). In control retinas, the Tubb3 domain was slightly smaller and included within the GFP domain (Fig. 3A, brackets 3A'). In *Neurog2* mutants, the Tubb3 domain was decreased (Fig. 3B), with a greater separation between the leading edge of Tubb3+ cells and the peripheral extent of the *Neurog2*^{GFP} domain (brackets, Fig. 3B'). To quantify the peripheral spread of neurogenesis, we measured the outer length of the Tubb3 and GFP domains in matched central retinal sections (Fig. 3E). At E11.75, the Tubb3 domain was significantly reduced in *Neurog2* mutant retinas. In controls, the Tubb3 domain occupied 84.7 ± 2.5% of the GFP domain (31.4 ± 1.4% of total circumference), but in *Neurog2* mutants, the Tubb3 domain was only 34.8 ± 7.0% of the GFP domain (11.9 ± 2.3% of total circumference; Fig. 3F and not shown). We also noted reduced neurogenesis in the nasal half of the retina and ventral to the optic nerve (not shown). In addition to Tubb3, we also observed reduced p27/Kip1 and Pou4f2/Brn3b expression domains in the absence of *Neurog2* (Figs. 3I–J'). We conclude that *Neurog2* mutants exhibit a reduction in retinal neurogenesis concomitant with reduced RGC specification and cell cycle exit.

Intriguingly, *Atoh7* is not required to propagate the spread of neurogenesis, as the size of the Tubb3 domain was unaffected in the absence of *Atoh7* (Figs. 3C,C',F and not shown). Like *Neurog2* mutants, mice lacking both *Atoh7* and *Neurog2* had diminished expansion of Tubb3 in relation to both the GFP domain and total circumference, though not different from *Neurog2* single mutants (Figs. 3D,D',F). Therefore, *Atoh7* and *Neurog2* do not work synergistically to promote the propagation of neurogenesis. To investigate further, we assessed the percentage of differentiating neurons within the Tubb3 domain and observed fewer Tubb3+ cells in *Neurog2* mutants, *Atoh7* mutants, and double mutants compared to controls, again in a non-synergistic manner (Fig. 3G). Previous studies indicate that at E11.5 p27+ postmitotic retinal cells and Pou4f2+ RGCs are significantly reduced in *Atoh7* mutants (Le et al., 2006; Wang et al., 2001). Although *Atoh7* mutants do exhibit fewer p27+ cells, the peripheral extent of the p27 domain was not reduced (not shown). As expected, the Pou4f2/Brn3b-expressing cells were virtually absent in *Atoh7* mutants and *Neurog2;Atoh7* double mutants (not shown). Thus, the expansion of neurogenesis requires *Neurog2*, but not *Atoh7*, although each is required to produce normal numbers of differentiating neurons.

The co-localization of *Neurog2* and *Atoh7* reporters and the reduced propagation of neurogenesis in *Neurog2* mutants from E11.0–E11.75 suggested that the peripheral spread of endogenous *Atoh7* might also be affected. Indeed, *Neurog2* mutants had a reduction in the width of the *Atoh7* mRNA expression domain at E11.75 (Figs. 3K,K'). Further, in the diencephalon, *Atoh7*-expressing cells were virtually absent in *Neurog2* mutants (arrows, Figs. 3K,K'). Another early bHLH factor, *Neurod1*, is required for normal amacrine, S-cone, and rod photoreceptor development (Inoue et al., 2002; Liu et al., 2008; Morrow et al., 1999). Although the *Neurod1* and *Atoh7* domains were the same width in controls, we did not observe any appreciable changes in the *Neurod1* expression domain in *Neurog2* mutant retinas (Figs. 3L,L'), consistent with a previous study (Akagi et al., 2004). Together, the outward spread of *Neurog2* specifically affects the expansion of *Atoh7* but is not required for its initial activation.

Delayed neurogenesis in Neurog2 mutants is restored

Neurog2 is required for the propagation, but not the initiation of neurogenesis, as a cluster of neural precursor cells appears in *Neurog2* mutants between E11.0–E11.75. Next, we analyzed retinal

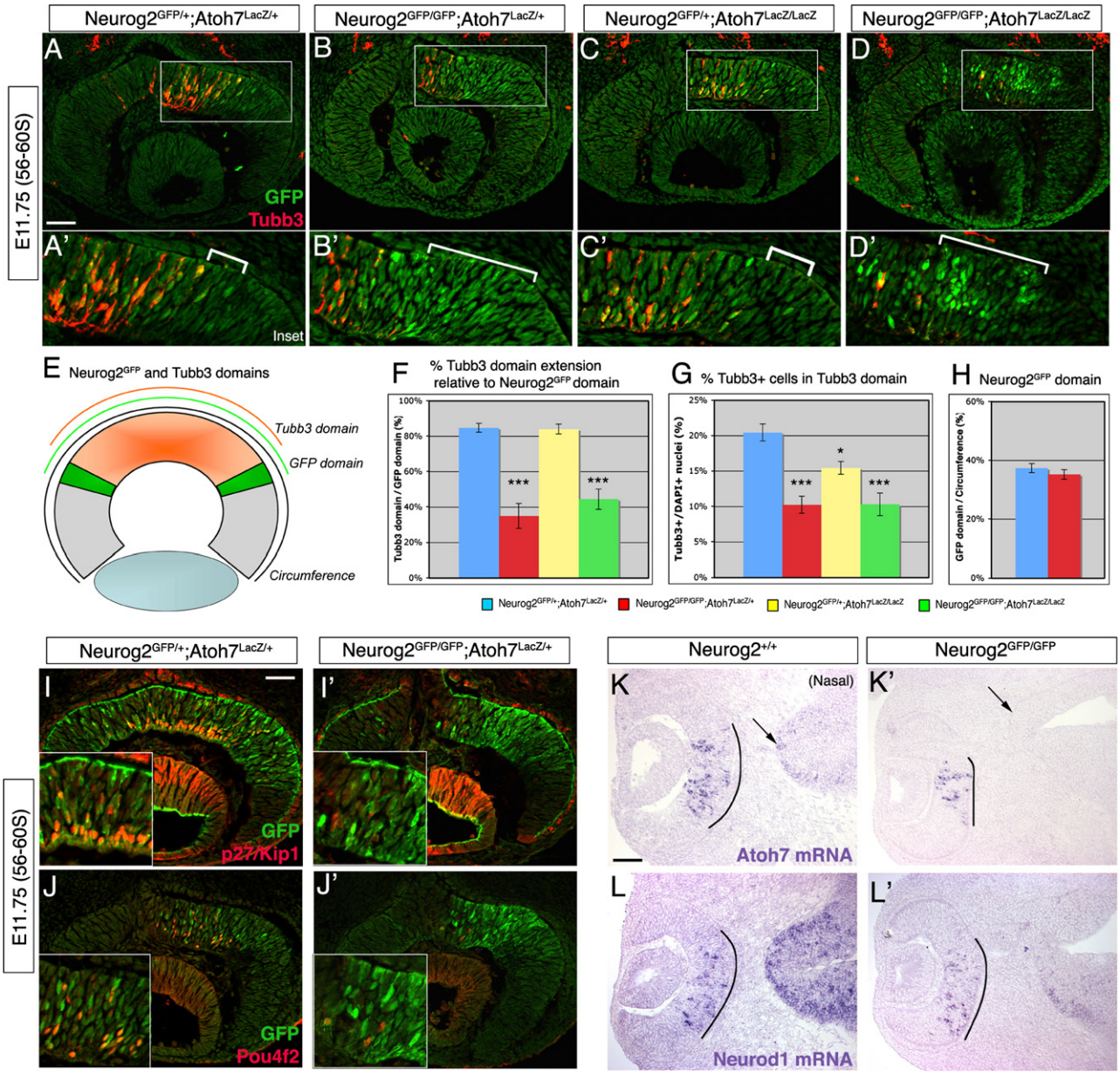

Fig. 3. Delay of early neurogenesis in *Neurog2* mutants. (A–D) Tubb3 and *Neurog2*^{GFP} labeling of double-heterozygote controls (A), *Neurog2*$^{GFP/GFP}$;*Atoh7*$^{LacZ/+}$ (*Neurog2* mutants) (B), *Neurog2*$^{GFP/+}$; *Atoh7*$^{LacZ/LacZ}$ (*Atoh7* mutants) (C), and double mutant (D) embryos at E11.75. (A'–D') Insets show higher magnification of the peripheral extent of Tubb3 expression, brackets mark GFP+/Tubb3− domain. (E) Measurement scheme for retinal circumference, Tubb3 and *Neurog2*^{GFP} expression domain widths. (F) Compared to controls, the Tubb3 domain was diminished relative to the *Neurog2*^{GFP} domain in *Neurog2* mutants and double mutants, but not in *Atoh7* mutants. (G) The percentage of Tubb3+ cells per total DAPI+ nuclei in the Tubb3 domain indicated that both *Neurog2* and *Atoh7* mutants had diminished neural differentiation. (H) The distal extent of GFP expression was the same in *Neurog2*$^{GFP/+}$ or *Neurog2*$^{GFP/GFP}$ eyes. (I–J') *Neurog2* mutants also exhibited a reduction of the p27/Kip1 (I,I') and Pou4f2/Brn3b (J,J') domains. (K–L') *Atoh7* (K,K') and *Neurod1* (L,L') mRNA expression in *Neurog2*$^{+/+}$ and *Neurog2*$^{GFP/GFP}$ retinas, indicated a smaller *Atoh7* domain, while *Neurod1* expression was unaffected. Scale bars: 50 μm in A,I,K. $^{*}p<0.05$, $^{***}p<0.001$; $n=6$ eyes (3 embryos) per genotype.

development in these mice from E12.0 to E15.5. From E12.0–E12.5, the Tubb3, p27/Kip1, and Pou4f2/Brn3b domains were truncated relative to the *Neurog2*^{GFP} domain (brackets, Figs. 4A,A' and not shown). We also noted reduced neurogenesis in the nasal half of the retina and ventral to the optic nerve (not shown), indicating that the progression of neurogenesis was affected in both central–peripheral and dorsal–ventral axes. However, by E13.5 the pattern of neurogenesis in *Neurog2* mutants was very similar to that of controls. In the temporal retina of both genotypes, the neurogenic domain extended to the periphery, to the border of the *Neurog2*^{GFP} domain (Figs. 4B,B'). On the nasal side, however, the Tubb3 and Pou4f2/Brn3b domains were still reduced relative to the GFP domain in *Neurog2* mutants (brackets, Figs. 4B,B' and not shown). By E15.5, the central to peripheral distribution of Tubb3+ or Pou4f2/Brn3b+ cells throughout the retina had caught up to that of controls (Figs. 4C,C' and not shown). Thus, neurogenesis and RGC specification are restored in *Neurog2* mutants, largely between E12.5 and E15.5.

Neurog2 and Atoh7 coordinate normal retinal size, but control distinct aspects of fate determination

At the initiation of retinal neurogenesis, *Neurog2* is required for the propagation of the *Atoh7* expression domain. Therefore, to test for cross-regulation or synergistic activities between *Neurog2* and *Atoh7*, we compared the four earliest retinal fates (RGCs, cone photoreceptors, amacrine and horizontal interneurons) in *Neurog2* and *Atoh7*

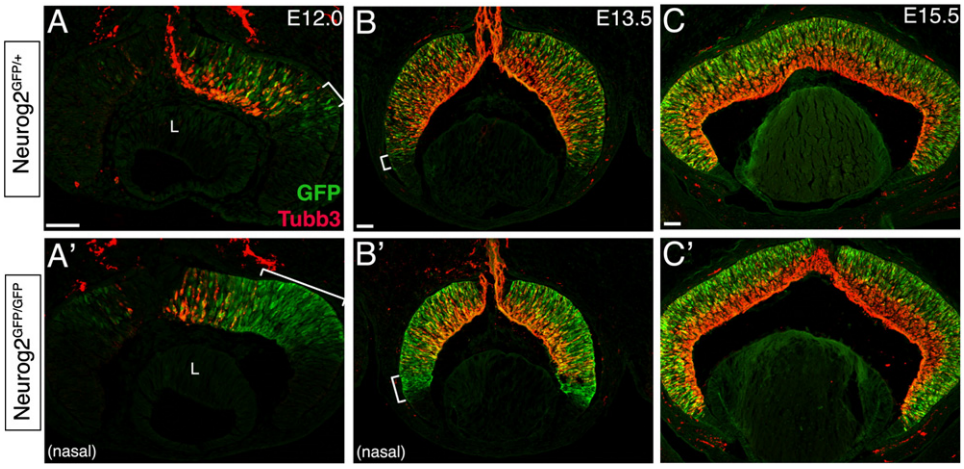

Fig. 4. Arrested neurogenesis in the absence of *Neurog2* is temporary. (A,A') At E12.0, the peripheral extent of the Tubb3 domain is reduced in *Neurog2*$^{GFP/GFP}$ retinas compared to controls (brackets, A,A'). (B,B') At E13.5, the peripheral extent of Tubb3 domain is reduced only on the nasal side of the optic cup, compared to the *Neurog2*^{GFP} domain (brackets). (C,C') By E15.5, the peripheral extent of Tubb3 expression was indistinguishable between *Neurog2* mutants and heterozygous controls. Scale bars: 50 μm in A,B,C; $n=8$ eyes (4 embryos) per genotype.

single and double mutants. Since the loss of *Neurog2* results in neonatal lethality, mutant mice were analyzed at P0.5.

First, we examined retinal thickness of single and double mutants (Figs. 5A–D,M). Adult *Atoh7* mutants have reduced laminar thickness (Brown et al., 2001; Brzezinski et al., 2005), already present at P0.5 (Figs. 5C,M). Compared to controls (Fig. 5A), *Neurog2* mutant mice also had significantly thinner retinas (Fig. 5B,M), similar to *Atoh7* mutants (Fig. 5C,M). Furthermore, *Neurog2;Atoh7* double mutant retinas were significantly reduced in thickness compared to both wild types and single mutants (Fig. 5D,M). This indicates that the loss of both *Neurog2* and *Atoh7* has an additive effect on retinal size, presumably representing synergistic or parallel roles in proliferation and/or survival during embryonic retinogenesis. To understand if reduced proliferation or increased cell death are responsible for the smaller retinas, we analyzed proliferating S-phase retinal progenitors by BrdU pulse-labeling cells, and apoptotic cells by activated Caspase-3 expression at several embryonic ages. *Atoh7* single mutants had no defect in proliferation or apoptosis at E15.5 (Le et al., 2006). At both E11.5 and E15.5, there was no difference in BrdU+ cells between wild type, *Neurog2* mutant, and *Neurog2;Atoh7* double mutant retinas (Figs. 6A–D and data not shown). The percentage of Caspase-3+ cells was normal in E15.5 *Neurog2*$^{-/-}$ eyes (Figs. 6E–H), as well as at E12.0 during the delay in neurogenesis (not shown). However, the number of apoptotic cells was significantly increased in *Neurog2;Atoh7* double mutants (Fig. 6H), suggesting an overlapping function for these bHLH factors in regulating some aspect of cell survival. Therefore, the increased apoptosis and enhanced reduction of retinal thickness were consistent with one another in double mutants.

To understand the extent by which the four early cell types might be altered in *Neurog2* mutants, we quantified RGCs, cones, horizontal and amacrine interneurons in P0.5 retinas. Although a loss of RGCs might be expected since their progression was delayed from E11.5–E13.5, we instead found a 2%±0.2% increase in Pou4f2+ RGCs within P0.5 *Neurog2* mutants (Fig. 5O). As expected, *Atoh7* and *Atoh7;Neurog2* double mutants had essentially no Pou4f2/Brn3b+ RGCs at this age (not shown). We conclude that although the percentages of RGCs in P0.5 *Neurog2* mutant eyes are significantly elevated, this phenotype cannot overcome the agenesis of RGCs in the absence of *Atoh7*.

Cone photoreceptors and Neurog2+ progenitor cells are significantly increased in *Atoh7* mutants (Brown et al., 2001; Brzezinski et al., 2005; Le et al., 2006), suggesting that cone photoreceptor genesis might normally be blocked by *Atoh7* indirect suppression of *Neurog2* expression. Analysis of single and double mutants (*Neurog2*$^{GFP/GFP}$; *Atoh7*$^{LacZ/LacZ}$) showed the trend of increased RXRγ+ cone precursor cells in the outer retinas of *Atoh7*$^{LacZ/LacZ}$ and double mutant mice (Figs. 5G,N). However, the loss of *Neurog2* alone (*Neurog2*$^{GFP/GFP}$) had no significant effect on the percentage of cone photoreceptors (Figs. 5F,N), nor did it enhance or suppress the percentages of cones in *Atoh7;Neurog2* double mutants (Figs. 5H,N). This suggests that although there is a simultaneously nonautonomous increase in cone photoreceptors and Neurog2+ cells in *Atoh7* mutants (Le et al., 2006), these are independent events that are likely to occur in separate populations of retinal progenitor cells.

Characterization of *Neurog2;Ascl1;Atoh3* and *Neurog2;Neurod1;Atoh3* triple mutant mice suggested a partial requirement for *Neurog2* during horizontal and amacrine interneuron differentiation (Akagi et al., 2004). To determine if the loss of *Neurog2* alone affects these cell types, we quantified the percentages of AP2α+ amacrine cells (arrow, Fig. 2O) (Yan and Wang, 2004) and Prox1+ cells, which give rise to a mixed population of horizontal and amacrine neurons (arrow, Fig. 2P) (Dyer et al., 2003). The AP2α protein (Figs. 5I–L,P–R) is expressed by both displaced amacrines in the GCL and amacrines that reside in the INL. We found normal distributions and percentages of AP2α+ amacrines in *Neurog2* single mutants (Figs. 5J,P–R). However, *Atoh7* single mutants, and the double mutants had significant increases in amacrines (Figs. 5K,L,P–R), consistent with a previous analysis of amacrines in *Atoh7* mutants (Wang et al., 2001). Finally, we compared the percentages of Prox1+ horizontals and amacrines (Figs. 5S–U). Here we observed only a significant increase in Prox1+ displaced amacrines in *Atoh7;Neurog2* double mutants (Figs. 5S–U). The different outcomes between Prox1+ and AP2α+ amacrines in *Atoh7* single and double mutants probably resulted because the Prox1+ population (0.8%) is such a small subset of AP2α+ amacrines (29%). Regardless, we conclude that *Neurog2* alone is not required for the specification of prenatal cone, amacrine and horizontal interneurons.

Ascl1 can compensate for the loss of Neurog2

Removal of *Neurog2* during embryonic retinal development results in a temporal delay of early retinal neurogenesis, which then returns to normal between E12.5–E15.5 (Fig. 4). Therefore, it is plausible that other factors, for example another bHLH proneural factor, compensate for the loss of *Neurog2* in the early retina. We tested several such candidates here. First, at E15.5 the patterns of *Atoh7* and *Neurod1* mRNA were indistinguishable in control and *Neurog2* mutants (not shown). If one of these factors compensates for the loss of *Neurog2*, we should have observed overexpression of *Atoh7* or *Neurod1*. Next, other *neurogenin* gene family members, *Neurog1* and *Neurog3*, are

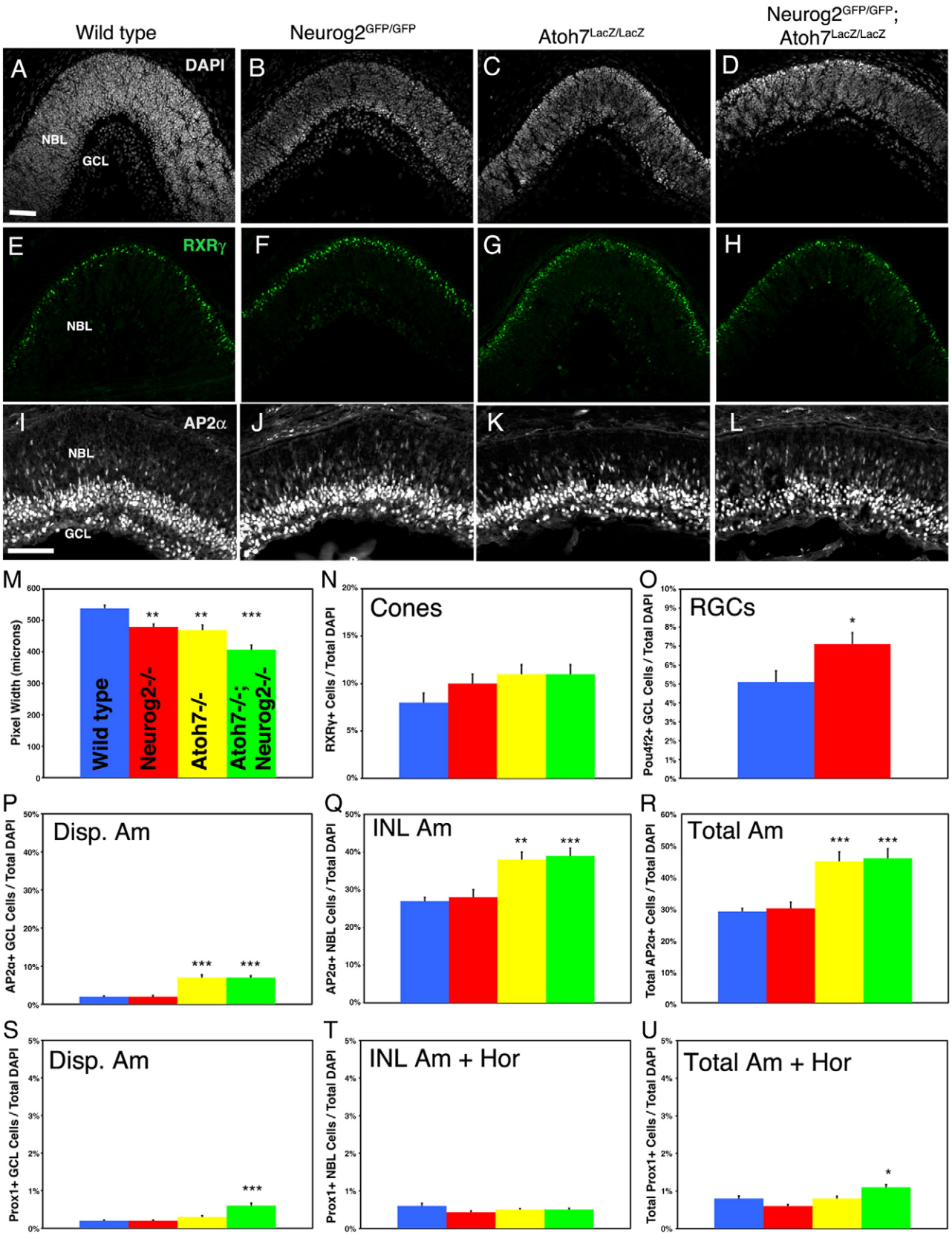

Fig. 5. Comparison prenatal retinal cell types in *Neurog2*, *Atoh7* and *Neurog2;Atoh7* double mutants. (A–D) Retinal thickness was measured as the vitreal–scleral width of DAPI+ nuclei in the NBL and GCL at P0.5. (E–H) Cone precursors were assessed by RXRγ labeling in the outer NBL. (I–L) AP2α+ amacrines in the forming INL and GCL. (M) Compared to wild type controls, *Neurog2* mutants and *Atoh7* mutants had reduced retinal thickness, and double mutants were significantly thinner than either single mutant. (N) No significant change in RXRγ+ cells was found in any genotype, although there was a trend towards increased cones in *Atoh7* mutants and double mutants. (O) *Neurog2* mutants had a small increase in Pou4f2+ RGCs. (P–R) AP2α+ amacrines were unaffected in *Neurog2* mutants, but significantly increased in *Atoh7* mutants and double mutants in both the GCL and NBL. (S–U) Prox1+ retinal cells we significantly increased in the GCL of *Neurog2;Atoh7* double mutants, but unaffected in *Neurog2* or *Atoh7* single mutants. Scale bar: 50 μm in A, I. $^{*}p<0.05$, $^{**}p<0.01$, $^{***}p<0.001$; $n=6$–8 eyes (3–4 P0.5 pups) per genotype. NBL = neuroblastic layer; GCL = ganglion cell layer.

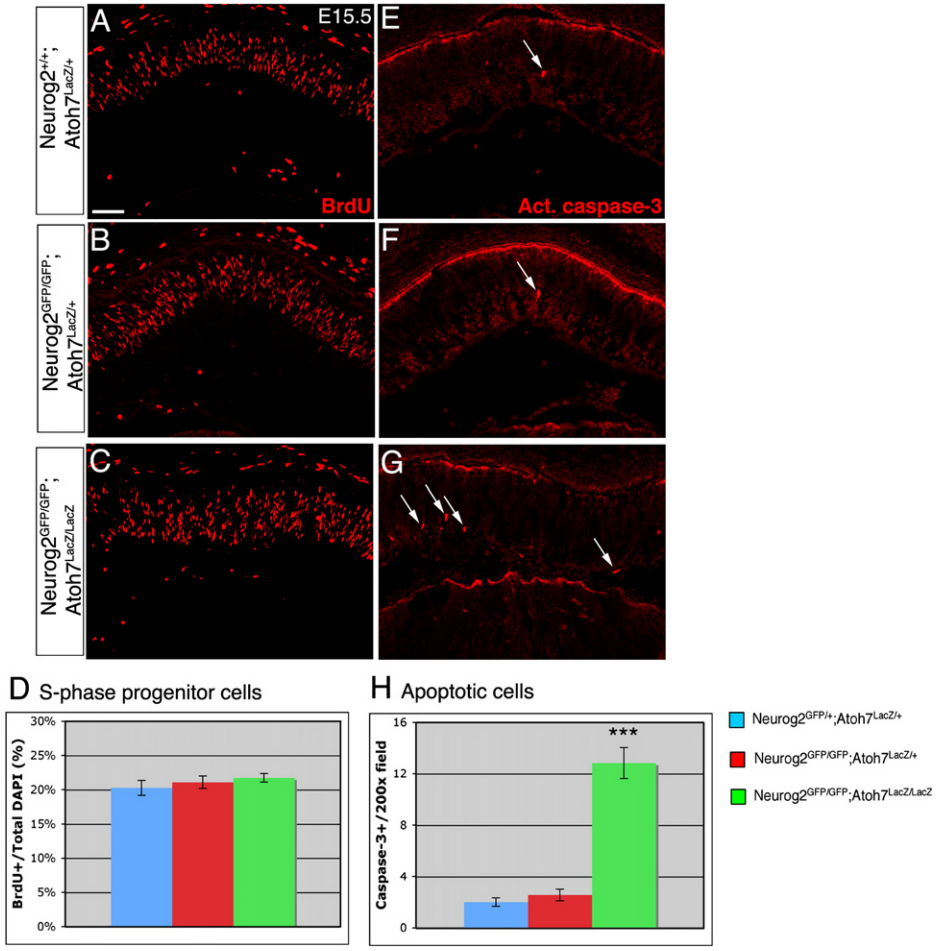

Fig. 6. Cell proliferation and apoptosis in the absence of *Neurog2*. (A–D) The percentage of BrdU+S-phase cells at E15.5 was normal in *Neurog2* mutants (*Neurog2*$^{GFP/GFP}$;*Atoh7*$^{LacZ/+}$) and double mutants (*Neurog2*$^{GFP/GFP}$;*Atoh7*$^{LacZ/LacZ}$). (E–H) The percentage of activated Caspase-3+ apoptotic cells (arrows in E–G) was significantly increased in double mutants, but not in *Neurog2* single mutants. Scale bar: 50 μm in A. ***$p<0.001$; $n=6$ eyes (3 embryos) per genotype.

expressed in the chick retina, but not that of frog (Ma et al., 2009; Nieber et al., 2009). So we asked whether either paralogue might be ectopically upregulated in *Neurog2* mutant eyes, but neither Neurog1 nor Neurog3 protein were detectable in E11.75–E15.5 control and *Neurog2*$^{-/-}$ retinas (not shown). Finally, we evaluated the onset of *Ascl1* expression in wild type retinas. In the E11.5 optic cup, *Ascl1* mRNA and protein are not expressed (Fig. 7I and data not shown), but beginning at early E12.5, a small population of Ascl1+ cells is detectable in the dorso-central retina (arrow, Fig. 7A). By E13.5, Ascl1 expression has spread outward to the peripheral and ventral poles of the retina (not shown). Therefore, the normal onset and progression of *Ascl1* expression coincides both spatially and temporally with the recovery of neurogenesis observed in *Neurog2* mutants from E12.5–E13.5.

The timing of these events suggested that *Ascl1* might be capable of restoring the delayed neurogenesis of *Neurog2* mutants. If so, then misexpression of *Ascl1* within the *Neurog2*-lineage should restore the peripheral expansion of retinal neurogenesis. To test this directly, we took advantage of the *Neurog2*^{Ascl1KI} allele, a homologous recombination of an IRES-*Ascl1* cassette into the endogenous *Neurog2* gene locus, thereby functionally replacing *Neurog2* with *Ascl1* (Fode et al., 2000). By mating *Neurog2*$^{Ascl1KI/+}$ and *Neurog2*$^{GFP/+}$ heterozygotes, *Neurog2*$^{GFP/Ascl1KI}$ embryos were generated, in which *Neurog2* function was removed and replaced by that of *Ascl1* within the *Neurog2*-lineage (Fode et al., 2000). At E12.0, both *Neurog2*$^{GFP/+}$ and *Neurog2*$^{GFP/GFP}$ retinas exhibited only rare Ascl1+ cells by immunofluorescence (Figs. 7A,A',A" and not shown), indicating that *Ascl1* is not precociously expressed in the absence of *Neurog2*. By contrast, *Neurog2*$^{GFP/Ascl1KI}$ retinas had abundant numbers of ectopic Ascl1+ cells (Figs. 7B,B',B"), most of which were also GFP+, indicating a substitution of *Ascl1* in cells that normally express *Neurog2*. We then compared the width of the Tubb3 and GFP domains in *Neurog2*$^{GFP/+}$, *Neurog2*$^{GFP/GFP}$, and *Neurog2*$^{GFP/Ascl1KI}$ embryonic retinas at E12.0. Strikingly, upon *Ascl1* replacement of *Neurog2*, the width of the Tubb3 + domain was now the same as in controls (Figs. 7C–E). To determine the effects of *Ascl1* on RGC differentiation, we similarly evaluated the Pou4f2/Brn3b expression domain in these three genotypes. Indeed, the width of the Pou4f2/Brn3b domain in *Neurog2*$^{GFP/Ascl1KI}$ retinas was identical to controls (Figs. 7F–H). Thus, although *Ascl1* normally activates in the retina after *Neurog2*, it is sufficient to rescue the block in the progression of early neurogenesis and RGC differentiation found in *Neurog2* mutant eyes.

Because progression of the *Atoh7* domain is initially delayed in *Neurog2* mutants from E11.75–E12.5 (Figs. 3K,K'), we asked whether *Ascl1* rescues the neurogenic wave via activation of *Atoh7*. The expression of *Atoh7* was compared among E11.5–E12.5 *Neurog2*$^{+/+}$, *Neurog2*$^{GFP/+}$, *Neurog2*$^{GFP/GFP}$ and *Neurog2*$^{GFP/Ascl1KI}$ litters (Figs. 7I–P and not shown). To verify the presence of ectopic *Ascl1*, its expression was monitored on adjacent sections from each embryo. At E11.5, *Neurog2*$^{GFP/Ascl1KI}$ optic cups had a reduced domain of *Atoh7* mRNA (compare Figs. 7K,L), but, ectopic *Ascl1* was not yet present (Figs. 7I,J). A day later at E12.5, when *Ascl1* is normally expressed by a few retinal cells, we found abundant ectopic expression in *Neurog2*$^{GFP/Ascl1KI}$ retinas (Figs. 7M,N), along with a normal pattern of *Atoh7* mRNA (Figs. 7O,P). Although ectopic *Ascl1* and *Atoh7* mRNA both appeared at E12.5, we do not think that rescue occurred at the level of *Atoh7*

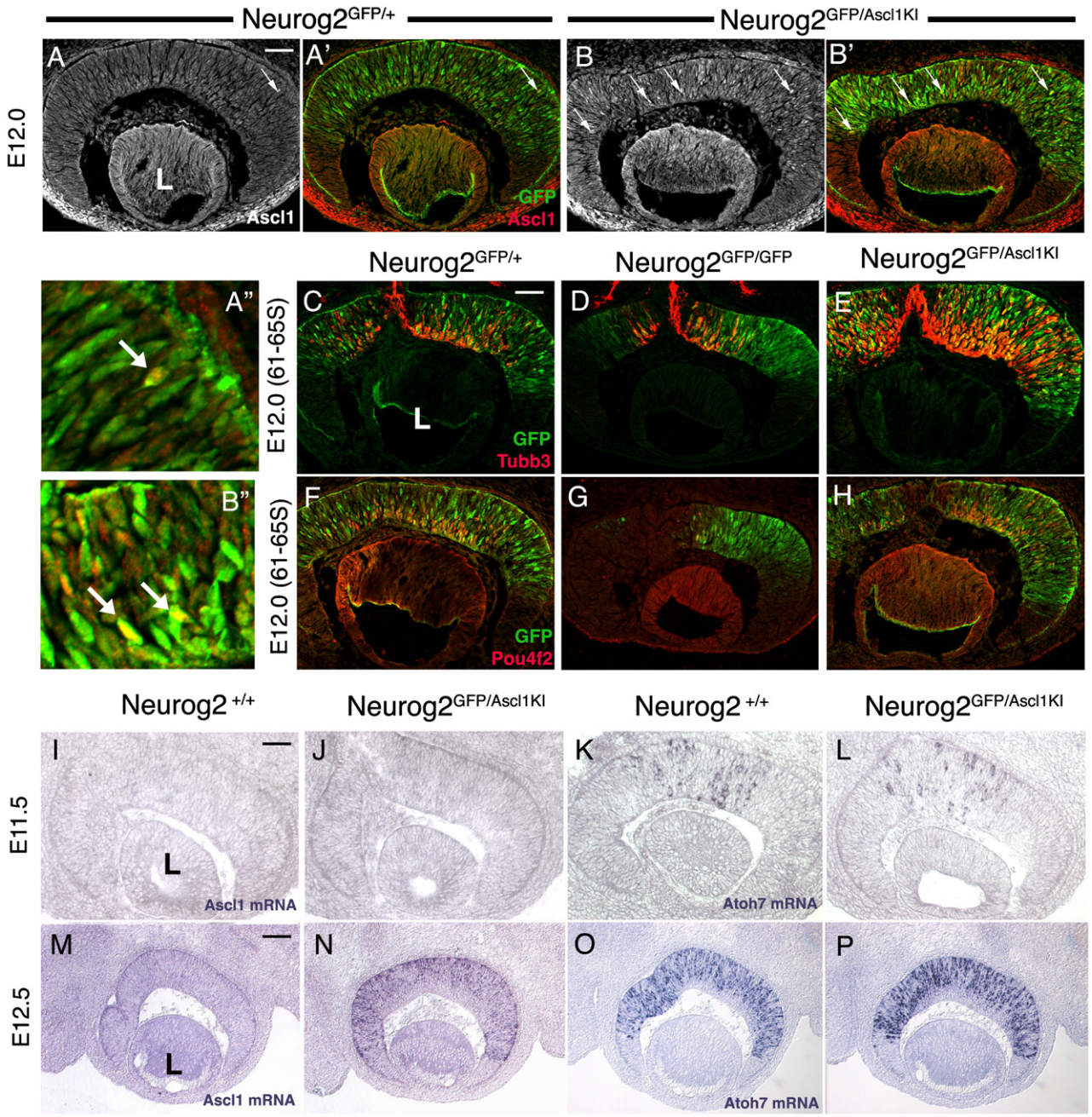

Fig. 7. *Ascl1* rescue of delayed neurogenesis in *Neurog2* mutants. (A,A') At E12.0, only rare Ascl1+ cells are present in *Neurog2*$^{GFP/+}$ eyes. The Ascl1+ cell in A coexpresses GFP, thus it is in the *Neurog2* lineage (arrow in A'. and higher magnification in A"). (B,B') *Neurog2*$^{GFP/Ascl1KI}$ retinas have many more Ascl1+GFP+ cells (arrows in B,B' and higher magnification in B"). (C–E) Tubb3 and GFP co-labeling at E12.0. Delayed progression of Tubb3+ neurons in *Neurog2*$^{GFP/GFP}$ mutants (D) was not found in *Neurog2*$^{GFP/Ascl1KI}$ eyes (E), which had an identical Tubb3 domain to controls (C). (F–H) Immunolabeling for Pou4f2/Brn3b and GFP showed that differentiated RGCs were also normal in *Neurog2*$^{GFP/Ascl1KI}$ mice (H), compared to *Neurog2*$^{GFP/GFP}$ mutants (G). (I–L) Ectopic *Ascl1* expression is delayed in *Neurog2* mutants, relative to endogenous Neurog2 expression (compare to Fig. 1), with a smaller domain of *Atoh7* mRNA expression in *Neurog2*$^{GFP/Ascl1KI}$ retinas (K,L). (M–P) At E12.5, ectopic *Ascl1* and normal *Atoh7* mRNA expression patterns are observed. Scale bars: 75 μm in A,C; 50 μm in I,M; $n = 3$–4 embryos per genotype; L = Lens.

transcriptional regulation. In support of this idea, the loss of *Ascl1* has no effect on *Atoh7* mRNA expression from E11.5 and E15.5 (Suppl. Figs. 1A–D), the Ascl1 protein does not bind to *Atoh7* 5′ regulatory DNA (Skowronska-Krawczyk et al., 2009), and *Drosophila* Scute and Atonal proteins have different E Box binding site consensus sequences (Powell et al., 2004). Somewhat paradoxically, at E17.5 *Ascl1* was proposed to suppress *Atoh7* (Akagi et al., 2004), although *Atoh7* upregulation was only found in the retinas of two bHLH triple mutant combinations that included *Ascl1* mutants. Furthermore, *Ascl1* and *Neurog2* mutually suppress each other's mRNA expression in the E17.5 retina (Akagi et al., 2004), which is somewhat at odds with the normal expression of *Ascl1* in E11.5–E15.5 *Neurog2* mutants (Suppl. Figs. 1E,F), and of Neurog2 GFP or protein in E11.5–E15.5 *Ascl1*$^{-/-}$ retinas (not shown). Although particular bHLH factors can suppress one another's expression at older stages of retinal formation, there is no evidence that these regulatory interactions are direct (Akagi et al., 2004). We hypothesize that late embryonic retinal bHLH cross suppression involves intermediate genes and/or occurs nonautonomously, particularly since these factors do not encode transcriptional repressors.

Discussion

Here, we investigated bHLH transcription factor expression and function during the initiation of retinogenesis in mouse, and identify *Neurog2* as one intrinsic regulator of the leading edge of neurogenesis. Onset and expansion of *Neurog2* and *Atoh7* expression predicts the initial wave front, concomitant with the compartmentalization of the neural retina and optic stalk by *Pax6* and *Pax2*, respectively. The first RGCs are subsequently specified in the dorso-central retina, and differentiation spreads ventrally and peripherally, similar to that found in fish and chick (Hu and Easter, 1999; Prada et al., 1991). *Neurog2* is required for the propagation of neurogenesis, and though its loss initially causes a dramatic phenotype, retinal neurogenesis becomes corrected in a few days. At P0.5, mutant retinas exhibited only a minor increase in RGCs, with no defect in cone, amacrine or horizontal neuron genesis. Interestingly, this recovery occurred during the onset and expansion of *Ascl1* expression, which was sufficient to correct the initial delay in RGC genesis.

Conservation of proneural bHLH function during initiation of murine retinal neurogenesis

The initial wave of retinal neurogenesis in mouse closely resembles the same process in non-mammalian vertebrate and *Drosophila* eyes. In fruit flies, a morphogenetic furrow sweeps across the eye imaginal disc from posterior to anterior ahead of retinal neurogenesis (Ready et al., 1976). At the anterior edge of the morphogenetic furrow, the bHLH protein *atonal* specifies the first ommatidial photoreceptor (R8) and promotes the progression of the morphogenetic furrow (Brown et al., 1995; Jarman et al., 1994, 1995). Like in *Drosophila*, the progression of neurogenesis in the vertebrate retina exhibits wave-like properties. In zebrafish, cells cease proliferation and adopt an RGC fate in a nasal-to-temporal sequence, determined by the *atonal*-orthologue *Ath5*/*lakritz* (Hu and Easter, 1999; Kay et al., 2001). In chick, RGC differentiation proceeds outward from the optic stalk, with a bias for the temporal half of the retina (McCabe et al., 1999; Prada et al., 1991). In chicken, *neurogenin2* and *Ath5* expression are present in the central retina at the onset of neurogenesis, and microarray profiling of mouse retinal progenitor cells identified a subpopulation with *Neurog2* and *Atoh7* mRNA coexpression (Trimarchi et al., 2008b). More recently, chick and mouse Ngn2/*Neurog2* were shown to activate directly the *Ath5*/*Atoh7* promoter, although the number of binding sites utilized differs between these two species (Matter-Sadzinski et al., 2001; Matter-Sadzinski et al., 2005; Skowronska-Krawczyk et al., 2009).

Here, we show that these *atonal* family members have distinct functions in mouse where *Neurog2* controls the propagation of neurogenesis, and *Atoh7* regulates RGC specification. Not surprisingly, together *Atoh7* and *Neurog2* reconstitute the orthologous roles of *atonal* in the *Drosophila* eye. Subdivisions of *atonal* functions during vertebrate development were already known, since the semi-orthologues *Atoh7* and *Atoh1* are present in mutually exclusive regions of the nervous system, thereby parsing *Drosophila atonal* functions within the mouse visual, auditory, and proprioceptive systems, respectively (Helms et al., 2000; Hufnagel et al., 2007; Saul et al., 2008).

Another example of functional subdivision relates to the ability of *Drosophila atonal* to autoregulate its own expression, which does not occur for the *Xenopus Ath5* or mouse *Atoh7* genes (Hutcheson et al., 2005; Riesenberg et al., 2009). Previously, *Atoh7* was reported to suppress *Neurog2* expression nonautonomously in the E13–15 retina (Le et al., 2006). Here, we found that the earliest *Atoh7*^{LacZ}+ cells are also in the *Neurog2*^{GFP} lineage, and that *Neurog2* is present in S-phase cells, slightly preceding *Atoh7* expression in these cells as they become newly postmitotic. We conclude that *Neurog2* is a positive regulator of *Atoh7* expression, since the peripheral expansion of *Atoh7* was delayed in *Neurog2* mutants. Thus, in mouse these two genes cross-regulate one another, but at different stages of retinal neurogenesis. During the initial propagation of neurogenesis, *Neurog2* directly activates *Atoh7* expression (this paper and Skowronska-Krawczyk et al., 2009), but several days later *Atoh7* nonautonomously suppresses *Neurog2* expression (Le et al., 2006). Importantly, like *atonal* autoregulation within committed R8 cells in the morphogenetic furrow, *Neurog2* cross-regulation of *Atoh7* is an integral part of wave front progression during the initiation of mammalian retinal neurogenesis.

Directing the wavefront of mammalian retinal neurogenesis

Neurog2 expression expands peripherally ahead of multiple markers of retinal neurogenesis. This small *Neurog2*^{GFP}+/Tubb3-negative domain likely contains Neurog2+ cells in S-phase. As these cells progress through the terminal mitosis, a subset of *Neurog2*^{GFP}+ cells express *Atoh7*, p27/Kip1 and Tubb3. Therefore, the spatial difference between the GFP+/Tubb3+ and peripheral GFP+/Tubb3-negative domains likely reflects the temporal difference in cell cycle status between differentiating neurons and proliferating progenitors poised to differentiate, respectively. This is also supported by Pou4f2/Brn3b onset more centrally in newly postmitotic RGCs. Hence, the outward spread of *Neurog2* expression demarcates the leading edge of neurogenesis, in which progenitor cells exit the cell cycle and become specified as retinal neurons, most of which differentiate as RGCs.

We predicted that BrdU+S-phase progenitors would be increased in E11.5 *Neurog2*$^{-/-}$ eyes, since there was an obvious reduction in p27/Kip1+ postmitotic cells. The correlation of these outcomes would indicate that *Neurog2* regulates retinal cell cycle progression, however this was not the case. It remains plausible that E11.5–E13.5 *Neurog2*$^{-/-}$ cells inappropriately accumulate in G2 phase. However, we currently favor a different possibility in which *Neurog2* mutant cells undergo transient changes in cell cycle length. Determining percentages of individual cell cycle markers at single time points would not uncover this defect. Instead, window labeling should be employed in the future to measure the cell cycle length of GFP+ retinal progenitors in *Neurog2*$^{GFP/+}$, *Neurog2*$^{GFP/GFP}$ and *Neurog2*$^{GFP/Ascl1KI}$ retinas. In this regard, *Ascl1* may uniquely rescue the *Neurog2* phenotype, since mitotically active retinal progenitors appear to only express these two bHLH factors during embryonic retinal neurogenesis. Moreover, *Neurod1* only partially rescues the *Atoh7* RGC phenotype, and *Atoh3* not at all (Mao et al., 2008), while *Ascl1* cannot rescue the *Atoh7* RGC phenotype (Hufnagel et al, in prep).

Extrinsic signal pathways, like *FGF* and *sonic hedgehog* (*shh*), direct key aspects of retinal patterning and neurogenesis (Martinez-Morales et al., 2005; McCabe et al., 1999; Neumann and Nuesslein-Volhard, 2000; Picker and Brand, 2005). A decade ago, *shh* was shown to propagate a retinal wave in the zebrafish retina (Neumann and Nuesslein-Volhard, 2000), but the mechanism for this subsequently underwent modification. *Ath5* expression and RGC genesis were shown to initiate normally in *sonic you* (*syu*) mutants (Kay et al., 2005; Masai et al., 2005). However, the period for the retinal wave to progress from nasal to temporal becomes extended when postmitotic retinal neurons are unable to secrete Shh. Therefore, retinal *shh* maintains progression but cannot initiate retinal neurogenesis. Instead, *shh* in the midline appears to trigger initiation of retinogenesis and *Ath5* expression. It is unknown if midline *shh* activates *Neurog2* in the zebrafish optic cup. In the mouse retina, activation and expansion of *Neurog2* and *Atoh7* expression precedes the appearance of retinal derived *shh* at E12.5 (Jensen and Wallace, 1997). In the future, it will be important to correlate the onset of midline and retinal *shh* with a) the time course of *Neurog2* expression, b) *Neurog2* regulation of early neurogenesis, c) the period when the delay is overcome in *Neurog2* mutants and d) the ability of *Ascl1* to rescue the *Neurog2* phenotype.

There are other signaling pathways that should be considered as well. For example, thyroid hormone signaling, which is important for photoreceptor differentiation, is deployed in multiple coordinated waves, at different phases of progenitor proliferation (Trimarchi et al., 2008a). Yet another example of extrinsic signaling is the *Notch* pathway, which also controls the timing of RGC differentiation and bHLH expression (Austin et al., 1995; Bao and Cepko, 1997; Nelson et al., 2006; Nelson and Reh, 2008).

Importantly in the chick eye, McCabe et al (1999) demonstrated that proximity to the wave front is not required for the progression of RGC genesis, indicating that this process depends more strongly on intrinsic components than extrinsic signals. Here, *Neurog2* retinal expression was correlated with and identified as required for the spatiotemporal progression of the wave of neurogenesis in the mouse eye. Potentially, *Neurog2* may act as a temporal integrator, interpreting combinations of extrinsic signals and multiple intrinsic inputs, from transcription factors such as *Pax6* and *Sox2* (Marquardt et al., 2001; Taranova et al., 2006), resulting in the activation and expansion of *Neurog2*, followed by neurogenic wave initiation. There is evidence for other intrinsic factor regulation of spatiotemporal progression of neurogenesis. In the *orJ* mouse, the loss of *Vsx2*/*Chx10*, which is critical for maintaining retinal progenitor proliferation, results in severe microphthalmia, lack of peripheral neurogenesis, and a delay in RGC-derived *shh* signaling (Bone-Larson et al., 2000; Burmeister et al., 1996; Sigulinsky et al., 2008). Although *Vsx2*/*Chx10* is ubiquitously expressed in retinal progenitors prior to the initiation of neurogenesis, it likely acts in concert with *Neurog2* and other factors to control the wave of neurogenesis in the retina. Another spatiotemporal process, cell migration is tightly coordinated for normal laminar patterning in the neocortex and retina — as cells exit the cell cycle and adopt a neural fate, they must migrate out of the ventricular zone to reach the proper layer. Recently, *Neurog2* and other proneural genes have been shown to regulate cortical migration, in part through regulation of *Rnd2*, a small GTP binding protein (Ge et al., 2006; Heng et al., 2008). Thus, coordinating spatiotemporal aspects of retinal development seems to require the tight coupling of multiple facets of neurogenesis by proneural bHLH and homeodomain transcription factors.

While *Neurog2* is necessary for the propagation of neurogenesis and *Atoh7* expression, it is not required for their initiation, clearly indicating that other factors are required. The initiation is neurogenesis is highly dependent on *Pax6*, critical for the expression of multiple bHLH factors (Brown et al., 1998; Marquardt et al., 2001; Riesenberg et al., 2009). The onset of proneural bHLH gene expression and retinal neurogenesis closely coincides with the downregulation of *Pax2* in the nascent neural retina, a known regulator of *Pax6* (Schwarz et al., 2000). It stands to reason, then, that the timing of bHLH initiation may be controlled indirectly by *Pax2* regulation of *Pax6* function or directly by *Pax2* repression of bHLH gene expression.

A bHLH network controlling retinal neurogenesis

In different contexts of the developing nervous system, *Neurog2* controls proliferation, cell cycle exit, cell fate identity, neurotransmitter specification, cell migration, axon guidance, and survival (Aaker et al., 2009; Britz et al., 2006; Cai et al., 2000; Fode et al., 1998, 2000; Seibt et al., 2003). However, previous to this study no phenotype was attributable solely to *Neurog2* function during vertebrate retinal development. Here, we uncovered a key role for *Neurog2* in regulating the initial progression of early retinal neurogenesis and RGC specification, which can be compensated for by substitution of *Ascl1* for *Neurog2*. Throughout the CNS, *Ascl1* and *Neurog2* are intricately linked in a context-dependent manner. In the forebrain, *Neurog2* represses *Ascl1* to maintain dorsal projection neuron identity, while in the dorsal neural tube *Neurog2* appears to function temporally downstream of *Ascl1* to influence the timing of cell cycle exit (Fode et al., 2000; Helms et al., 2005). Other *Neurog2*^{Ascl1KI} replacement experiments demonstrate that *Ascl1* cannot rescue the *Neurog2* phenotype in the dorsal forebrain or dorsal root ganglia (Fode et al., 2000; Parras et al., 2002), but can partially compensate for ventral spinal cord and midbrain dopaminergic neuron phenotypes (Kele et al., 2006; Parras et al., 2002).

In the retina, *Neurog2* and *Ascl1* both appear to promote cell cycle exit and neuronal determination analogously, such that *Ascl1* expressed from the *Neurog2* locus can rescue the temporal delay of RGC genesis. This was unexpected, since RGCs are unaffected in *Ascl1* mutants, and *Ascl1* is thought to function primarily in specification of later-born retinal fates, particularly rod photoreceptors and bipolar interneurons (Hatakeyama et al., 2001; Tomita et al., 1996). Here we propose that the normal onset of endogenous *Ascl1* expression activates a subsequent wave of neurogenesis. In *Neurog2* mutants, retinal second wave cells could either autonomously produce first wave and second wave neurons, or nonautonomously jumpstart the stalled first wave cells. The absence of increased retinal cell proliferation in *Neurog2* mutants suggests the first scenario as the least likely. At present there is no hard evidence for *Ascl1* regulation of a subsequent wave, although *Ascl1* impressively rescues the *Neurog2* phenotype. To settle this question, the *Ascl1* retinal lineage and mutant phenotypes (ideally with a conditional allele) will need careful examination during prenatal retinogenesis.

Conversely, *Ascl1* may compensate for the loss of *Neurog2* by an unknown mechanism. Interestingly, *Ascl1* performs a critical function during zebrafish retinal regeneration (Fausett et al., 2008). Both *Neurog2* and *Ascl1* are present in proliferating neural progenitor cells (Jasoni and Reh, 1996; Yan et al., 2001), implying that they share a common set of downstream target genes critical for controlling cell cycle progression versus exit for neural differentiation. The expression of *Neurog2* and *Ascl1* at different times during retinogenesis seems integral with their context-specific functions. Intriguingly, the removal of both *Neurog2* and *Ascl1* did not result in the total loss of neurogenesis or *Atoh7* expression (Akagi et al., 2004), suggesting that further levels of compensation exist. In postnatal *Ascl1* mutant retinas, horizontal interneuron and rod photoreceptor differentiation is temporarily reduced (Tomita et al., 1996), potentially restored by yet another compensatory factor. Overall, we conclude that the spatial and temporal progression of mammalian retinal neurogenesis is regulated by the bHLH factor *Neurog2*, and that a remarkable compensatory potential exists in the developing retina, potentially through a secondary wave of neurogenesis directed by *Ascl1*.

Acknowledgments

The authors thank François Guillemot for *Neurog2*^{GFP} and *Neurog2*^{Ascl1KI} mice; Kenny Campbell for *Ascl1* embryonic litters; David Anderson and Masato Nakafuku for Neurog2 antibodies; Jane Johnson for Ascl1 antibody; Lev Prasov and Tom Glaser for helpful discussions, and Kenny Campbell, Masato Nakafuku, Brian Gebelein, Steve Woods, and Noah Shroyer for critical comments. This work was supported by the Edith J. Crawley Memorial Scholars Program, University of Cincinnati Department of Ophthalmology (RBH), and NIH grants EY13612 and EY18097 (NLB).

Appendix A. Supplementary data

Supplementary data associated with this article can be found, in the online version, at doi:10.1016/j.ydbio.2010.02.002.

References

Aaker, J.D., Patineau, A.L., Yang, H.J., Ewart, D.T., Gong, W., Li, T., Nakagawa, Y., McLoon, S.C., Koyano-Nakagawa, N., 2009. Feedback regulation of NEUROG2 activity by MTGR1 is required for progression of neurogenesis. Mol. Cell. Neurosci. 42, 267–277.

Akagi, T., Inoue, T., Miyoshi, G., Bessho, Y., Takahashi, M., Lee, J.E., Guillemot, F., Kageyama, R., 2004. Requirement of multiple basic helix–loop–helix genes for retinal neuronal subtype specification. J. Biol. Chem. 279, 28492–28498.

Altshuler, D.M., Turner, D.L., Cepko, C.L., 1991. Specification of cell type in the vertebrate retina. In: Lam DM-K, S.C. (Ed.), Cell Lineage and Cell Fate in Visual System Development. MIT Press, Cambridge, MA, pp. 37–58.
Austin, C.P., Feldman, D.E., Ida Jr., J.A., Cepko, C.L., 1995. Vertebrate retinal ganglion cells are selected from competent progenitors by the action of Notch. Development 121, 3637–3650.
Bao, Z.Z., Cepko, C.L., 1997. The expression and function of Notch pathway genes in the developing rat eye. J. Neurosci. 17, 1425–1434.
Baumer, N., Marquardt, T., Stoykova, A., Spieler, D., Treichel, D., Ashery-Padan, R., Gruss, P., 2003. Retinal pigmented epithelium determination requires the redundant activities of Pax2 and Pax6. Development 130, 2903–2915.
Bone-Larson, C., Basu, S., Radel, J.D., Liang, M., Perozek, T., Kapousta-Bruneau, N., Green, D.G., Burmeister, M., Hankin, M.H., 2000. Partial rescue of the ocular retardation phenotype by genetic modifiers. J. Neurobiol. 42, 232–247.
Brittis, P.A., Meiri, K., Dent, E., Silver, J., 1995. The earliest patterns of neuronal differentiation and migration in the mammalian central nervous system. Exp. Neurol. 134, 1–12.
Britz, O., Mattar, P., Nguyen, L., Langevin, L.M., Zimmer, C., Alam, S., Guillemot, F., Schuurmans, C., 2006. A role for proneural genes in the maturation of cortical progenitor cells. Cereb. Cortex 16 (Suppl 1), i138–i151.
Brown, N.L., Kanekar, S., Vetter, M.L., Tucker, P.K., Gemza, D.L., Glaser, T., 1998. Math5 encodes a murine basic helix–loop–helix transcription factor expressed during early stages of retinal neurogenesis. Development 125, 4821–4833.
Brown, N.L., Patel, S., Brzezinski, J., Glaser, T., 2001. Math5 is required for retinal ganglion cell and optic nerve formation. Development 128, 2497–2508.
Brown, N.L., Sattler, C.A., Paddock, S.W., Carroll, S.B., 1995. Hairy and emc negatively regulate morphogenetic furrow progression in the *Drosophila* eye. Cell 80, 879–887.
Brzezinski, J.A., 2005. The Role of Math5 in Retinal Development. PhD thesis in Human Genetics. University of Michigan, Ann Arbor, MI.
Brzezinski, J.A., Brown, N.L., Tanikawa, A., Bush, R.A., Sieving, P.A., Vitaterna, M.H., Takahashi, J.S., Glaser, T., 2005. Loss of circadian photoentrainment and abnormal retinal electrophysiology in Math5 mutant mice. Invest. Ophthalmol. Vis. Sci. 46, 2540–2551.
Burmeister, M., Novak, J., Liang, M.Y., Basu, S., Ploder, L., Hawes, N.L., Vidgen, D., Hoover, F., Goldman, D., Kalnins, V.I., Roderick, T.H., Taylor, B.A., Hankin, M.H., McInnes, R.R., 1996. Ocular retardation mouse caused by Chx10 homeobox null allele: impaired retinal progenitor proliferation and bipolar cell differentiation. Nat. Genet. 12, 376–384.
Cai, L., Morrow, E.M., Cepko, C.L., 2000. Misexpression of basic helix–loop–helix genes in the murine cerebral cortex affects cell fate choices and neuronal survival. Development 127, 3021–3030.
Dyer, M.A., Cepko, C.L., 2001. p27Kip1 and p57Kip2 regulate proliferation in distinct retinal progenitor cell populations. J. Neurosci. 21, 4259–4271.
Dyer, M.A., Livesey, F.J., Cepko, C.L., Oliver, G., 2003. Prox1 function controls progenitor cell proliferation and horizontal cell genesis in the mammalian retina. Nat. Genet. 34, 53–58.
Easter Jr., S.S., 2000. Let there be sight. Neuron 27, 193–195.
Fausett, B.V., Gumerson, J.D., Goldman, D., 2008. The proneural basic helix–loop–helix gene ascl1a is required for retina regeneration. J. Neurosci. 28, 1109–1117.
Fode, C., Gradwohl, G., Morin, X., Dierich, A., LeMeur, M., Goridis, C., Guillemot, F., 1998. The bHLH protein NEUROGENIN 2 is a determination factor for epibranchial placode-derived sensory neurons. Neuron 20, 483–494.
Fode, C., Ma, Q., Casarosa, S., Ang, S.L., Anderson, D.J., Guillemot, F., 2000. A role for neural determination genes in specifying the dorsoventral identity of telencephalic neurons. Genes Dev. 14, 67–80.
Ge, W., He, F., Kim, K.J., Blanchi, B., Coskun, V., Nguyen, L., Wu, X., Zhao, J., Heng, J.I., Martinowich, K., Tao, J., Wu, H., Castro, D., Sobeih, M.M., Corfas, G., Gleeson, J.G., Greenberg, M.E., Guillemot, F., Sun, Y.E., 2006. Coupling of cell migration with neurogenesis by proneural bHLH factors. Proc. Natl. Acad. Sci. U. S. A. 103, 1319–1324.
Gowan, K., Helms, A.W., Hunsaker, T.L., Collisson, T., Ebert, P.J., Odom, R., Johnson, J.E., 2001. Crossinhibitory activities of Ngn1 and Math1 allow specification of distinct dorsal interneurons. Neuron 31, 219–232.
Hatakeyama, J., Tomita, K., Inoue, T., Kageyama, R., 2001. Roles of homeobox and bHLH genes in specification of a retinal cell type. Development 128, 1313–1322.
Helms, A.W., Abney, A.L., Ben-Arie, N., Zoghbi, H.Y., Johnson, J.E., 2000. Autoregulation and multiple enhancers control Math1 expression in the developing nervous system. Development 127, 1185–1196.
Helms, A.W., Battiste, J., Henke, R.M., Nakada, Y., Simplicio, N., Guillemot, F., Johnson, J.E., 2005. Sequential roles for Mash1 and Ngn2 in the generation of dorsal spinal cord interneurons. Development 132, 2709–2719.
Heng, J.I., Nguyen, L., Castro, D.S., Zimmer, C., Wildner, H., Armant, O., Skowronska-Krawczyk, D., Bedogni, F., Matter, J.M., Hevner, R., Guillemot, F., 2008. Neurogenin 2 controls cortical neuron migration through regulation of Rnd2. Nature 455, 114–118.
Holt, C.E., Bertsch, T.W., Ellis, H.M., Harris, W.A., 1988. Cellular determination in the *Xenopus* retina is independent of lineage and birth date. Neuron 1, 15–26.
Horton, S., Meredith, A., Richardson, J.A., Johnson, J.E., 1999. Correct coordination of neuronal differentiation events in ventral forebrain requires the bHLH factor MASH1. Mol. Cell. Neurosci. 14, 355–369.
Hu, M., Easter, S.S., 1999. Retinal neurogenesis: the formation of the initial central patch of postmitotic cells. Dev. Biol. 207, 309–321.
Hufnagel, R.B., Riesenberg, A.N., Saul, S.M., Brown, N.L., 2007. Conserved regulation of Math5 and Math1 revealed by Math5-GFP transgenes. Mol. Cell. Neurosci. 36, 435–448.
Hutcheson, D.A., Hanson, M.I., Moore, K.B., Le, T.T., Brown, N.L., Vetter, M.L., 2005. bHLH-dependent and -independent modes of Ath5 gene regulation during retinal development. Development 132, 829–839.
Inoue, T., Hojo, M., Bessho, Y., Tano, Y., Lee, J.E., Kageyama, R., 2002. Math3 and NeuroD regulate amacrine cell fate specification in the retina. Development 129, 831–842.
Jarman, A.P., Grell, E.H., Ackerman, L., Jan, L.Y., Jan, Y.N., 1994. Atonal is the proneural gene for *Drosophila* photoreceptors. Nature 369, 398–400.
Jarman, A.P., Sun, Y., Jan, L.Y., Jan, Y.N., 1995. Role of the proneural gene, atonal, in formation of *Drosophila* chordotonal organs and photoreceptors. Development 121, 2019–2030.
Jasoni, C.L., Reh, T.A., 1996. Temporal and spatial pattern of MASH-1 expression in the developing rat retina demonstrates progenitor cell heterogeneity. J. Comp. Neurol. 369, 319–327.
Jensen, A.M., Wallace, V.A., 1997. Expression of Sonic hedgehog and its putative role as a precursor cell mitogen in the developing mouse retina. Development 124, 363–371.
Kanekar, S., Perron, M., Dorsky, R., Harris, W.A., Jan, L.Y., Jan, Y.N., Vetter, M.L., 1997. Xath5 participates in a network of bHLH genes in the developing *Xenopus* retina. Neuron 19, 981–994.
Kay, J.N., Finger-Baier, K.C., Roeser, T., Staub, W., Baier, H., 2001. Retinal ganglion cell genesis requires lakritz, a Zebrafish atonal Homolog. Neuron 30, 725–736.
Kay, J.N., Link, B.A., Baier, H., 2005. Staggered cell-intrinsic timing of ath5 expression underlies the wave of ganglion cell neurogenesis in the zebrafish retina. Development 132, 2573–2585.
Kele, J., Simplicio, N., Ferri, A.L., Mira, H., Guillemot, F., Arenas, E., Ang, S.L., 2006. Neurogenin 2 is required for the development of ventral midbrain dopaminergic neurons. Development 133, 495–505.
Le, T.T., Wroblewski, E., Patel, S., Riesenberg, A.N., Brown, N.L., 2006. Math5 is required for both early retinal neuron differentiation and cell cycle progression. Dev. Biol. 295, 764–778.
Lee, M.K., Tuttle, J.B., Rebhun, L.I., Cleveland, D.W., Frankfurter, A., 1990. The expression and posttranslational modification of a neuron-specific beta-tubulin isotype during chick embryogenesis. Cell Motil. Cytoskeleton 17, 118–132.
Levine, E.M., Close, J., Fero, M., Ostrovsky, A., Reh, T.A., 2000. p27(Kip1) regulates cell cycle withdrawal of late multipotent progenitor cells in the mammalian retina. Dev. Biol. 219, 299–314.
Liu, H., Etter, P., Hayes, S., Jones, I., Nelson, B., Hartman, B., Forrest, D., Reh, T.A., 2008. NeuroD1 regulates expression of thyroid hormone receptor 2 and cone opsins in the developing mouse retina. J. Neurosci. 28, 749–756.
Lo, L., Dormand, E., Greenwood, A., Anderson, D.J., 2002. Comparison of the generic neuronal differentiation and neuron subtype specification functions of mammalian achaete-scute and atonal homologs in cultured neural progenitor cells. Development 129, 1553–1567.
Ma, W., Wang, S.Z., 2006. The final fates of neurogenin2-expressing cells include all major neuron types in the mouse retina. Mol. Cell. Neurosci. 31, 463–469.
Ma, W., Yan, R.T., Mao, W., Wang, S.Z., 2009. Neurogenin3 promotes early retinal neurogenesis. Mol. Cell. Neurosci. 40, 187–198.
Macdonald, R., Barth, K.A., Xu, Q., Holder, N., Mikkola, I., Wilson, S.W., 1995. Midline signalling is required for Pax gene regulation and patterning of the eyes. Development 121, 3267–3278.
Mao, C.A., Wang, S.W., Pan, P., Klein, W.H., 2008. Rewiring the retinal ganglion cell gene regulatory network: Neurod1 promotes retinal ganglion cell fate in the absence of Math5. Development 135, 3379–3388.
Marquardt, T., Ashery-Padan, R., Andrejewski, N., Scardigli, R., Guillemot, F., Gruss, P., 2001. Pax6 is required for the multipotent state of retinal progenitor cells. Cell 105, 43–55.
Martinez-Morales, J.R., Del Bene, F., Nica, G., Hammerschmidt, M., Bovolenta, P., Wittbrodt, J., 2005. Differentiation of the vertebrate retina is coordinated by an FGF signaling center. Dev. Cell 8, 565–574.
Masai, I., Stemple, D.L., Okamoto, H., Wilson, S.W., 2000. Midline signals regulate retinal neurogenesis in zebrafish. Neuron 27, 251–263.
Masai, I., Yamaguchi, M., Tonou-Fujimori, N., Komori, A., Okamoto, H., 2005. The hedgehog–PKA pathway regulates two distinct steps of the differentiation of retinal ganglion cells: the cell-cycle exit of retinoblasts and their neuronal maturation. Development 132, 1539–1553.
Matter-Sadzinski, L., Matter, J.M., Ong, M.T., Hernandez, J., Ballivet, M., 2001. Specification of neurotransmitter receptor identity in developing retina: the chick ATH5 promoter integrates the positive and negative effects of several bHLH proteins. Development 128, 217–231.
Matter-Sadzinski, L., Puzianowska-Kuznicka, M., Hernandez, J., Ballivet, M., Matter, J.M., 2005. A bHLH transcriptional network regulating the specification of retinal ganglion cells. Development 132, 3907–3921.
McCabe, K.L., Gunther, E.C., Reh, T.A., 1999. The development of the pattern of retinal ganglion cells in the chick retina: mechanisms that control differentiation. Development 126, 5713–5724.
Mori, M., Ghyselinck, N.B., Chambon, P., Mark, M., 2001. Systematic immunolocalization of retinoid receptors in developing and adult mouse eyes. Invest. Ophthalmol. Vis. Sci. 42, 1312–1318.
Morrow, E.M., Furukawa, T., Lee, J.E., Cepko, C.L., 1999. NeuroD regulates multiple functions in the developing neural retina in rodent. Development 126, 23–36.
Nelson, B.R., Gumuscu, B., Hartman, B.H., Reh, T.A., 2006. Notch activity is downregulated just prior to retinal ganglion cell differentiation. Dev. Neurosci. 28, 128–141.
Nelson, B.R., Reh, T.A., 2008. Relationship between Delta-like and proneural bHLH genes during chick retinal development. Dev. Dyn. 237, 1565–1580.
Neumann, C.J., Nuesslein-Volhard, C., 2000. Patterning of the zebrafish retina by a wave of sonic hedgehog activity. Science 289, 2137–2139.
Nieber, F., Pieler, T., Henningfeld, K.A., 2009. Comparative expression analysis of the neurogenins in *Xenopus tropicalis* and *Xenopus laevis*. Dev. Dyn. 238, 451–458.
Ohsawa, R., Kageyama, R., 2008. Regulation of retinal cell fate specification by multiple transcription factors. Brain Res. 1192, 90–98.

Parras, C.M., Schuurmans, C., Scardigli, R., Kim, J., Anderson, D.J., Guillemot, F., 2002. Divergent functions of the proneural genes Mash1 and Ngn2 in the specification of neuronal subtype identity. Genes Dev. 16, 324–338.
Perron, M., Boy, S., Amato, M.A., Viczian, A., Koebernick, K., Pieler, T., Harris, W.A., 2003. A novel function for Hedgehog signalling in retinal pigment epithelium differentiation. Development 130, 1565–1577.
Perron, M., Opdecamp, K., Butler, K., Harris, W.A., Bellefroid, E.J., 1999. X-ngnr-1 and Xath3 promote ectopic expression of sensory neuron markers in the neurula ectoderm and have distinct inducing properties in the retina. Proc. Natl. Acad. Sci. U. S. A. 96, 14996–15001.
Picker, A., Brand, M., 2005. Fgf signals from a novel signaling center determine axial patterning of the prospective neural retina. Development 132, 4951–4962.
Poggi, L., Vitorino, M., Masai, I., Harris, W.A., 2005. Influences on neural lineage and mode of division in the zebrafish retina in vivo. J. Cell Biol. 171, 991–999.
Powell, L.M., Zur Lage, P.I., Prentice, D.R., Senthinathan, B., Jarman, A.P., 2004. The proneural proteins Atonal and Scute regulate neural target genes through different E-box binding sites. Mol. Cell. Biol. 24, 9517–9526.
Prada, C., Puga, J., Perez-Mendez, L., Lopez And, R., Ramirez, G., 1991. Spatial and temporal patterns of neurogenesis in the chick retina . Eur. J. NeuroSci. 3, 1187.
Ready, D.F., Hanson, T.E., Benzer, S., 1976. Development of the *Drosophila* retina, a neurocrystalline lattice. Dev. Biol. 53, 217–240.
Riesenberg, A.N., Le, T.T., Willardsen, M.I., Blackburn, D.C., Vetter, M.L., Brown, N.L., 2009. Pax6 regulation of Math5 during mouse retinal neurogenesis. Genesis 47, 175–187.
Rodieck, R.W., 1998. The First Steps in Seeing. Sinauer, Sunderland, MA.
Saul, S.M., Brzezinski, J.A.T., Altschuler, R.A., Shore, S.E., Rudolph, D.D., Kabara, L.L., Halsey, K.E., Hufnagel, R.B., Zhou, J., Dolan, D.F., Glaser, T., 2008. Math5 expression and function in the central auditory system. Mol. Cell. Neurosci. 37, 153–169.
Schwarz, M., Cecconi, F., Bernier, G., Andrejewski, N., Kammandel, B., Wagner, M., Gruss, P., 2000. Spatial specification of mammalian eye territories by reciprocal transcriptional repression of Pax2 and Pax6. Development 127, 4325–4334.
Seibt, J., Schuurmans, C., Gradwhol, G., Dehay, C., Vanderhaeghen, P., Guillemot, F., Polleux, F., 2003. Neurogenin2 specifies the connectivity of thalamic neurons by controlling axon responsiveness to intermediate target cues. Neuron 39, 439–452.
Sidman, R., 1961. Histogenesis of mouse retina studied with thymidine-H3. In: Smelser, G. (Ed.), Structure of the Eye. Academic Press, New York, pp. 487–506.
Sigulinsky, C.L., Green, E.S., Clark, A.M., Levine, E.M., 2008. Vsx2/Chx10 ensures the correct timing and magnitude of Hedgehog signaling in the mouse retina. Dev. Biol. 317, 560–575.
Skowronska-Krawczyk, D., Chiodini, F., Ebeling, M., Alliod, C., Kundzewicz, A., Castro, D., Ballivet, M., Guillemot, F., Matter-Sadzinski, L., Matter, J.M., 2009. Conserved regulatory sequences in Atoh7 mediate non-conserved regulatory responses in retina ontogenesis. Development 136, 3767–3777.
Taranova, O.V., Magness, S.T., Fagan, B.M., Wu, Y., Surzenko, N., Hutton, S.R., Pevny, L.H., 2006. SOX2 is a dose-dependent regulator of retinal neural progenitor competence. Genes Dev. 20, 1187–1202.
Tomita, K., Nakanishi, S., Guillemot, F., Kageyama, R., 1996. Mash1 promotes neuronal differentiation in the retina. Genes Cells 1, 765–774.
Trimarchi, J.M., Harpavat, S., Billings, N.A., Cepko, C.L., 2008a. Thyroid hormone components are expressed in three sequential waves during development of the chick retina. BMC Dev. Biol. 8, 101.
Trimarchi, J.M., Stadler, M.B., Cepko, C.L., 2008b. Individual retinal progenitor cells display extensive heterogeneity of gene expression. PLoS ONE 3, e1588.
Wallace, V.A., Raff, M.C., 1999. A role for Sonic hedgehog in axon-to-astrocyte signalling in the rodent optic nerve. Development 126, 2901–2909.
Wang, S.W., Kim, B.S., Ding, K., Wang, H., Sun, D., Johnson, R.L., Klein, W.H., Gan, L., 2001. Requirement for math5 in the development of retinal ganglion cells. Genes Dev. 15, 24–29.
Willardsen, M.I., Suli, A., Pan, Y., Marsh-Armstrong, N., Chien, C.B., El-Hodiri, H., Brown, N.L., Moore, K.B., Vetter, M.L., 2009. Temporal regulation of Ath5 gene expression during eye development. Dev. Biol. 326, 471–481.
Xiang, M., Zhou, L., Peng, Y.W., Eddy, R.L., Shows, T.B., Nathans, J., 1993. Brn-3b: a POU domain gene expressed in a subset of retinal ganglion cells. Neuron 11, 689–701.
Yan, R.T., Ma, W.X., Wang, S.Z., 2001. neurogenin2 elicits the genesis of retinal neurons from cultures of nonneural cells. Proc. Natl. Acad. Sci. U. S. A. 98, 15014–15019.
Yan, R.T., Wang, S.Z., 2004. Requirement of neuroD for photoreceptor formation in the chick retina. Invest. Ophthalmol. Vis. Sci. 45, 48–58.
Yang, Z., Ding, K., Pan, L., Deng, M., Gan, L., 2003. Math5 determines the competence state of retinal ganglion cell progenitors. Dev. Biol. 264, 240–254.
Young, R.W., 1985. Cell differentiation in the retina of the mouse. Anat. Rec. 212, 199–205.